Engineering Structures 316 (2024) 118558

Contents lists available at ScienceDirect

Engineering Structures

journal homepage: www.elsevier.com/locate/engstruct

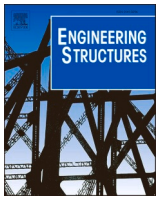

Capacity design assessment of composite reduced web section (RWS) connections

Fahad Falah Almutairi [a], Konstantinos Daniel Tsavdaridis [b,*]

[a] School of Civil Engineering, Faculty of Engineering and Physical Sciences, University of Leeds, Woodhouse Lane, LS2 9JT Leeds, UK
[b] Department of Engineering, School of Science & Technology, City, University of London, Northampton Square, EC1V 0HB London, UK

ARTICLE INFO

Keywords:
Capacity design
RWS connection
Ductility
Composite action
Retrofit

ABSTRACT

A gap in current design approaches demands explicitly introducing a capacity design approach when designing steel-concrete composite reduced web section (RWS) connections. This paper addresses this gap by presenting test-validated finite element models and parametric investigations, focusing on the presence and absence of composite action over the web opening, the diameter, and the end-distance of the web opening. Additionally, the first-ever comprehensive experimental and numerical database from the literature on bare steel and composite RWS connections is compiled and thoroughly analysed to develop the capacity design assessment for such connections. Both parametric investigations and the database highlight the significance of the capacity design ratio between the connected components in achieving a desirable ductile mechanism. This is crucial, as evidenced by the results: a 15 % increase in the connection's moment capacity led to an average 21 % difference in dissipated energy, favouring the web opening with a diameter of $50d_o$ over $80d_o$, in RWS connections with the presence of composite action. The results show that proper consideration of the capacity design approach in designing RWS connections ensures a stable yield mechanism is developed, resulting in the redistribution of global action and capping deformation demands on non-ductile elements. This enhances connections' rotational capacity and ductility by forming the Vierendeel mechanism. Lastly, the paper presents a detailing recommendation for employing RWS connections in both existing and new structures for seismic purposes.

1. Introduction

Different plastic failure mechanisms can manifest in steel moment-resisting frame (MRF) systems. These mechanisms depend on the relative strengths of beams, connections (i.e., end-plates), and columns (including panel zones) framing into a joint. These components of a joint can dissipate hysteretic energy through cyclic plastic deformations, providing that bolts and welding failures cannot be tolerated during earthquakes [1–4]. To this end, capacity design and ductility design employ a combination of i) components with high strength, and ii) components with high plastic deformation capacity to optimise the response of the MRF. This approach involves linking a favourable failure mechanism to a responsible component to provide the needed hysteretic energy dissipation. Other elements with comparable strength are then protected to ensure elastic behaviour. Experimental and numerical campaigns of EQUALJOINTS and EQUALJOINTS-Plus, projects validated the effectiveness of capacity design criteria in achieving desired joint responses [1–3,5,6]. Depending on the contribution of each component of the joint to the plastic failure mechanisms, a connection could be designed as being full, equal (balanced) or partial-strength, with or without any resultant yielding of the web panel.

It is generally acknowledged that beams are primary dissipative elements in MRFs, adhering to the 'strong column-weak beam' concept, which is an application of the capacity design criteria. In line with this concept, reduced web section (RWS) connections - where the material is removed from the web, have been demonstrated to enhance energy dissipation through the yielding of the perforated section [7–15]. The response mechanism of RWS connections, acting as two partial beams above and below the opening (top and bottom Tee-sections), induces four plastic hinges in the vicinity of the web opening (aka Vierendeel Mechanism, VM), as shown in Fig. 1. This mechanism can overcome challenges relate to the potential impact of composite action within the protected zone (steel area around the web or flange reduction) that could compromise the 'strong column-weak beam' design concept, and, thereby, causing an asymmetric yield moment mechanism. The former can lead to weak columns (story mechanism), while the latter can induce

* Corresponding author.
E-mail address: konstantinos.tsavdaridis@city.ac.uk (K.D. Tsavdaridis).

https://doi.org/10.1016/j.engstruct.2024.118558
Received 9 February 2024; Received in revised form 15 May 2024; Accepted 1 July 2024

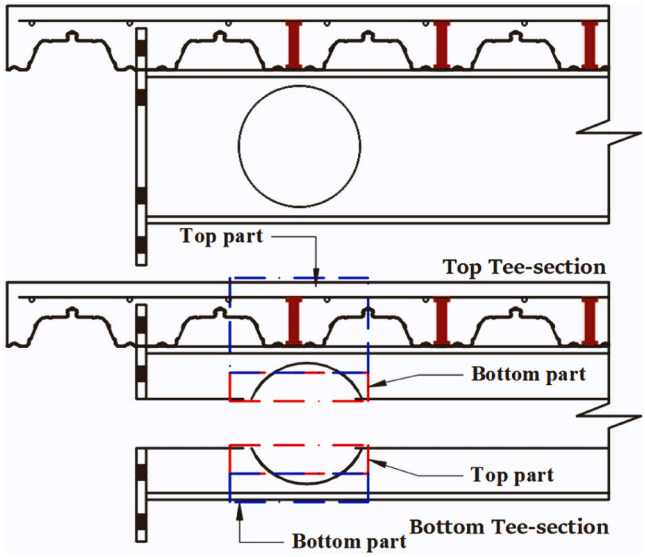

Fig. 1. Tee-sections of the perforated beam (two partial beams).

excessive strain demands on the beam's bottom flange.

Still, RWS connections face criticism because having web openings in high-shear zones is considered undesirable in seismic areas, as it may cause a non-ductile failure due to tearing and out-of-plane buckling. This is due to the resultant reduction in shear strength. The seismic design generally favours a shear strength higher than moment strength since it deteriorates much faster than its moment counterpart. In other words, capacity design principles aim to ensure that the shear resistance is larger than the demands induced by plastic mechanisms to prevent tearing and other fragile failure modes. The incorporation of a single web opening introduces three key failure modes: (1) shear failure because of the reduction in the shear capacity, (2) flexural failure because of the reduction in moment capacity, and (3) Vierendeel mechanism [23]. These modes are influenced by the web openings' shapes, sizes and locations [18,24]. Moreover, the reduction in load-carrying capacity is dependent on the type of loading, the geometry of the beam, and the shear-to-moment interaction at the centreline of the web opening [25–27]. Chung et al. observed that both shear failure and the Vierendeel mechanism may coincide around the web opening [16,17]. The Vierendeel mechanism is a local vertical shear failure that physically manifests when the steel reaches its yield capacity at the Tee-section ends (i.e., the formation of four plastic hinges) due to a couple of local shear forces. High shear forces and a large critical length of the opening are required to promote such a ductile Vierendeel mechanism and cap deformation demands on non-ductile elements [9,17,18]. Therefore, the failure mode of the perforated section could be controlled by adjusting the web opening shape, location and size [11,16–22]. Thus, the mechanism of RWS connections is to reduce the shear capacity of the section by creating a web opening in order to leverage the high shear forces to induce a Vierendeel (ductile) failure mode.

Recent experimental and numerical studies presented on traditional and demountable steel-concrete composite RWS connections with a diameter of web opening (d_o) equal to 80 % of the beam section's depth (h) near the connections in the high shear zone [7,8]. Notably, these studies exceed the limitations set by SCI-P355 guidance that states $d_o \leq 0.8h$ with a minimum depth of Tees ≥ flange thickness + 30 mm [26], by suppressing the minimum depth of Tees. Despite this, the Vierendeel mechanism governed the failure of all tested RWS connections [7], yet met the seismic requirements of ANSI/AISC 358–16, ANSI/AISC 341–16 and Eurocode 8 [28–30].

Another consideration, which forms the primary focus of this paper, is the fact that the current design approaches of RWS connections for seismic purposes overlooked the significant effect of a capacity design to ensure a stable yield mechanism is governed. The studies of Almutairi et al. [7,8] highlighted the importance of capacity design in the evolution of RWS connections to maximise the full benefit of the ductile mechanism while still adhering to the 'strong column-weak beam' concept. The studies also noted that introducing a web opening can re-classify a connection from partial to full strength. This is due to the reduction in the strength of the connected steel beam section. Such insights are crucial for retrofitting existing buildings and for guiding designs of new structures, potentially eliminating the need for thicker end-plate or stiffeners in extended end-plate connections.

Over the past decade, there has been a strong push towards the development of robust guidance, numerical models and acceptance criteria for the design and promotion of the use of RWS connections in MRFs in areas predisposed to seismic events [7,8,10,11,18,21,22,31–36]. This extensive research has resulted in patents and software developments [11,21,35–40]. Given the significance and continuity of this work, it is necessary to provide a comprehensive understanding of the key parameters, besides the size and location of the web opening, that influence the cyclic response of RWS connections, either with or without a composite slab. The focus of this paper is to assess how the capacity design ratio affects the response of both bare-steel and steel-concrete composite RWS connections in terms of ductility, energy dissipation, and equivalent viscous damping. To accomplish this, experimental and numerical databases are developed within this paper and existing literature for assessing the capacity design ratio on the response of the RWS connections. A gap in current design approaches demands explicitly introducing a capacity design approach when designing RWS connections. By integrating and extrapolating this data, this paper contributes to a more robust and expansive understanding of RWS connections, supporting the development of improved design practices and standards in seismic engineering.

2. Methodology

The establishment of benchmarks for seismic non-linear modelling is essential, as is setting acceptance criteria and reliably predicting the cyclic degradation effects and properties of RWS connections. These steps are crucial to assist researchers and engineers in integrating these properties into analysis tools. This endeavour should be extended by developing a comprehensive database of RWS connections, drawing from existing literature, both experimentally and numerically. Unfortunately, many of the studies within the existing literature were individual efforts, leading to a scarcity of test and FE details. This is further compounded by the lack of availability or preservation of full hysteretic moment-rotation curves for public access.

Physical testing is an efficient method, although it comes with high costs and is time-consuming. FE analysis offers acceptable and practical alternatives. However, FE analysis still requires physical testing for benchmarking to be employed for further investigations. There are limited experimental tests on RWS connections available for synthesis or evaluating the robustness of design guidelines and existing numerical models. Thus, an empirical study is needed to develop a database on bare steel and steel-concrete composite RWS connections. This database aids in verifying the assumptions and observations made during the numerical and experimental investigations. Such a database is valuable for researchers and engineers as it allows them to refine the existing models and contribute to developing and validating design codes and standards.

As such, this paper presents two main databases to identify similar trends illustrated in Fig. 2. This paper begins with i) high-fidelity FE models developed to simulate the structural behaviour of the four demountable composite RWS connections that were conducted by Almutairi et al. [7]. Along with leveraging two FE models validated in the companion paper [8], ii) a parametric study using New Zealand steel section profiles, the same as those used in the Chaudhari et al. tests, was conducted. This was a significant shift from the previous parametric

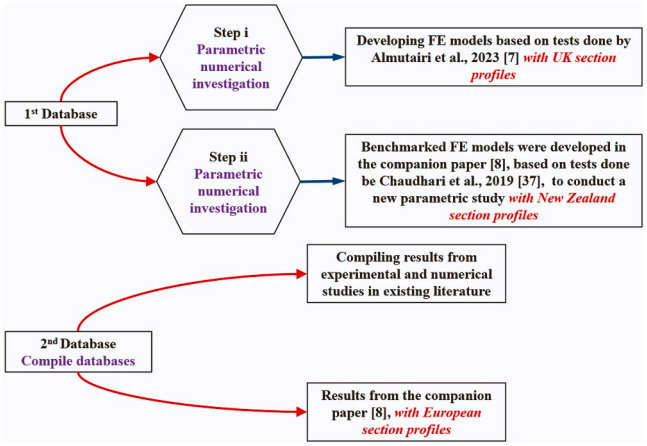

Fig. 2. Flow diagram to illustrate the methodology.

study's approach in the companion paper [8], where the European section profiles were used. The rationale for reverting to New Zealand sections was to enrich and diversify the existing database, thereby broadening the range of steel sections analysed and facilitating a more comprehensive analysis of RWS connection behaviours. The first database (i.e., i and ii) were analysed together which served as a reliable starting point for assessing the response of single-sided and double-sided RWS connections.

Lastly, the second database is a comprehensive compilation and extrapolation of both experimental and numerical non-dimensionalised results from existing literature along with results derived from the companion paper [8] (employing European sections). This effort was aimed at further investigating the characteristics of RWS connections to identify similar trends in comparison to the parametric numerical database presented in Section 4 in this study.

3. Deduction of response parameters of RWS connections

The Ibarra–Medina–Krawinkler (IMK) model [42] was employed in this study to consistently assess selected response (both strength and deformation) parameters influencing the cyclic response of RWS connections. In cases where full moment-rotation (**M-θ**) curves are absent in the literature (i.e., the assembled RWS connections database Section 5), both strength and deformation parameters as shown in Fig. 3, were sourced from the tabulated results in the literature. Fig. 3 illustrates the stages of defining the following strength and deformation parameters of the IMK model [42]:

- The elastic (K_e), strain-hardening (K_s) and post-capping (K_c) stiffnesses.
- The effective yield moment (M_{ye}) and its corresponding rotation (θ_y).
- The maximum moment resistance (M_m) and its corresponding rotation (θ_m).
- The ultimate moment (M_u) and its corresponding rotation (θ_u).

In this study, the ultimate moment strength (M_u) represents the moment of the last cycle in cases where the strength degradation occurs. If skeleton **M-θ** curves do not experience strength degradation, M_u would be equal to the maximum moment strength (M_m).

4. Parametric numerical investigation

4.1. Numerical validation

Numerical simulations were constructed using the nonlinear FEA programme ABAQUS [43]. These simulations are based on the numerical models developed by the first author in companion studies [8] as shown in Fig. 4. The capability of the numerical models to simulate the responses of both bare steel and traditional steel-concrete composite BEEPs with and without stiffeners, using the experimental results of Chaudhari et al. [41], has been previously validated in [8]. Similar numerical techniques have been employed to validate the findings of the

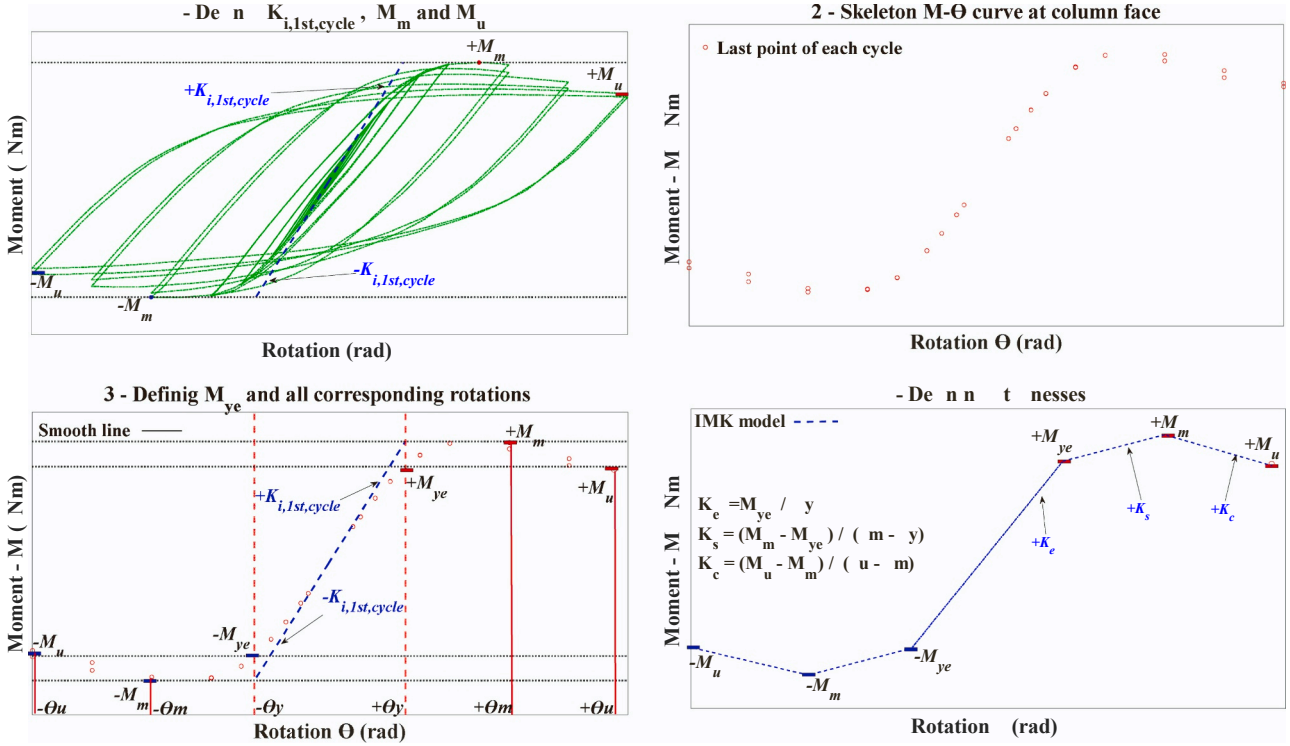

Fig. 3. Defining the strength and deformation parameters of IMK model.

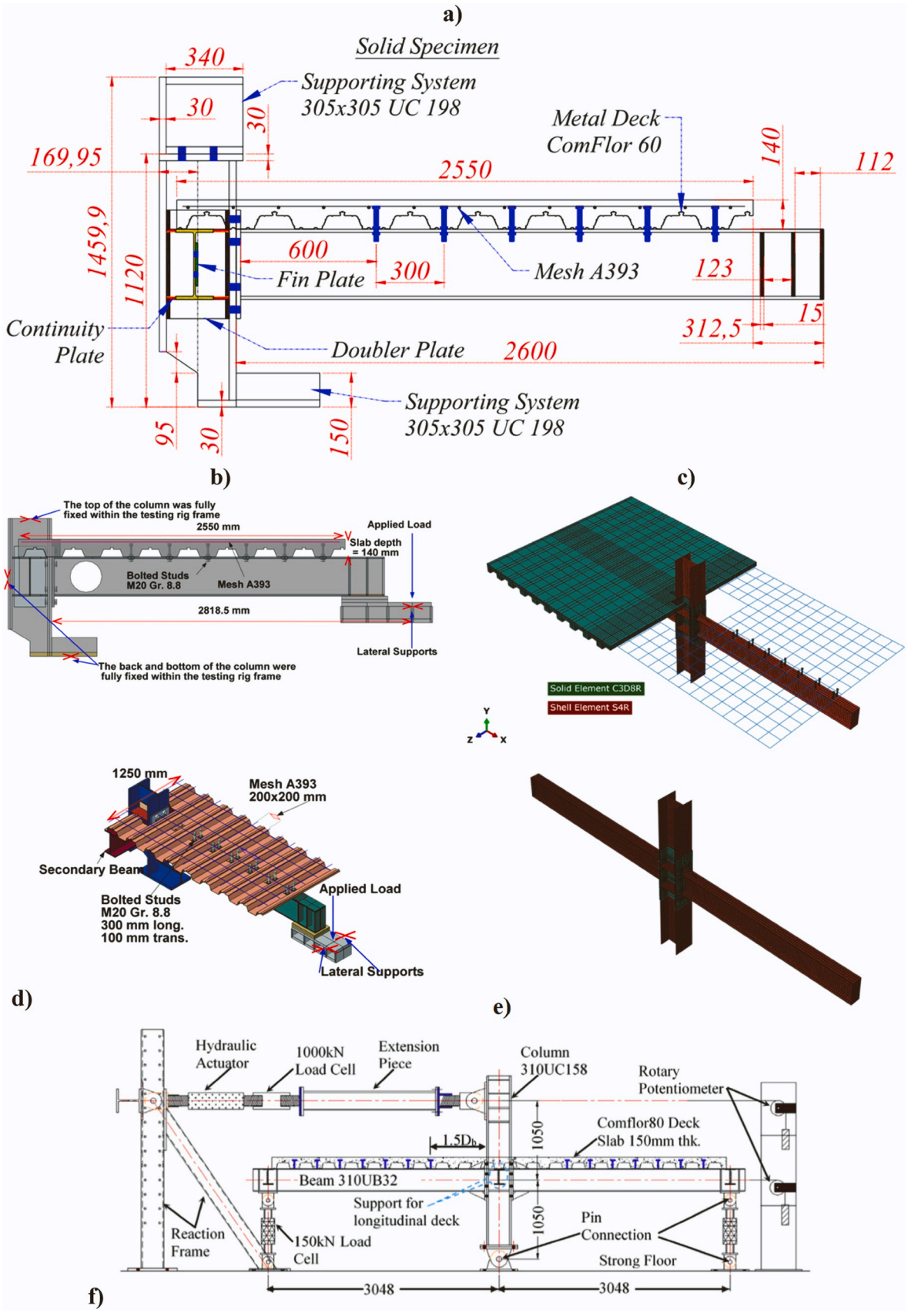

Fig. 4. Test set-ups and FE model for tests of [7] on the left and tests of [41] on the right.

cyclic testing of demountable steel-concrete composite BEEPs RWS connections by Almutairi et al. [7]. For the sake of completeness and convenience, a brief description of the numerical models is presented herein. A total of six experimental specimens were benchmarked by reproducing results of experimental investigations [7,41] (Table 1).

Numerical simulation techniques were defined to best replicate the hysteretic behaviour observed in the experimental findings (Fig. 5). These techniques also aimed to reduce analysis running time and conserve computer storage without compromising the accuracy of the results. In the numerical simulations, a combination of shell (S4R) and solid elements (C3D8R) with reduced integration was employed. S4R were adopted for beams, columns, plates and metal decks and C3D8R were utilised for concrete slabs, bolts, and welded or bolted shear studs. The steel rebars were represented using truss elements (T3D2), which can only carry uniaxial tension and compression.

Tie constraints were employed to simulate the welding between steel-to-steel elements. Normal and tangent interactions were applied to replicate the contact and friction between steel-to-steel elements (column, bolts and extended end-plates). This was achieved by defining a hard contact and adopting a friction coefficient equal to 0.2, which corresponds to the case of untreated rolled surfaces according to Eurocode 3 [44] as shown in Fig. 5. Additionally, a finite sliding approach was allowed for such contacts. A tie contact was applied between the reinforced concrete slab and metal deck to avoid numerical instabilities leading to early termination of the numerical simulation. The steel rebars as well as the welded and bolted shear studs were embedded into the concrete section. Fig. 6.

Eigenbuckling analyses initially were performed before the main analyses (Fig. 7). The first modes were scaled by the recommended factor of $t_w/200$ in accordance with [45] to introduce geometric imperfections accounting for typical local manufacturing tolerances. A combined non-linear material model that accounts for both isotropic and kinematic hardening of the material was adopted. An isotropic bi-linear material model with strain-hardening was employed for metal decks and steel rebars. The average values of coupon tests were utilised. In instances where tensile test results for certain steel elements were missing, the nominal values of material properties were taken from the manufacturer's specifications. The ultimate strains (εu) were equal to $15\varepsilon y$ and $10\varepsilon y$ for steel elements and bolts, respectively. The ultimate strain of bolted shear studs was equal to $10\varepsilon y$ as well. The rupture strain (εr) was designated as 0.2 for all steel elements and 0.05 for the bolts and bolted shear studs. The ductile damage option was employed by ABAQUS [43] to account for the effect of cracks that occurred in the vicinity of the web opening during the experimental tests [7].

The concrete damage plasticity (CDP) model was considered to model the tensile and compressive behaviours of concrete. The constitutive law defined in Eurocode 2 [46], along with the exponential tension softening model [47], were adopted to replicate the concrete crushing and cracking, respectively. Compression cylinder tests were used for concrete with axial tensile strength f_t and assumed to be 10 % of compressive strength of f_{ck}.

The boundary and loading conditions of experimental tests [7,41], including the gravity load, were incorporated into the numerical simulations (Fig. 8). Moreover, the "Bolt Load" option [43] was applied to simulate the tightening of bolts and bolted studs. The distribution of residual stresses, derived from testing the solid specimen, was accounted for in the numerical simulation of RWS-L-retrofit. This was done to mimic the effects of moderate seismicity for rehabilitation purposes [7].

The mesh sensitivity study was performed to best replicate the hysteretic behaviour of the experimental tests [7,41]. Such a study aimed to conserve storage space and to ensure that the analysis running time was maintained between 11 and 15 h on the High-Performance Computer. The mesh sizes for steel, slab, bolts and bolted studs were equal to 30, 50, and 7.5 mm, respectively. A mesh size equal to 20 mm, was selected for the main beams with a distance equal to 600 mm near the connection, as high concentrations of stresses/strains were expected.

The responses of numerical models compared to the experimental tests are depicted in Figs. 9–11. The numerical findings closely matched the hysteretic responses of the composite specimens with both welded and bolted shear studs, as well as the bare steel connection. The high accuracy between the numerical models and the experimental tests was evident in terms of both sagging and hogging capacities, stiffnesses, and, notably, in relation to cyclic and in-cycle deterioration up to the onset of fracture. The validated numerical models were utilised for conducting parametric assessments, generating a synthetic RWS database for further investigations.

4.2. Parameters

In Europe, the adoption of partial-strength connections is permissible provided that their ductility and rotational capacity are experimentally verified according to Eurocode 8 [30]. The recent EQUALJOINTS and EQUALJOINTS-Plus projects have produced seismic design criteria for such connections [1–3,5,6]. Such connections are cost-effective, with extended end-plate joints being about 30 % cheaper than full-strength, thereby reducing post-earthquake repair costs [6]. Nonetheless, full-strength connections are often preferred as they obviate the need for the experimental verification requirements of Eurocode 8 [30]. Recent studies by Almutairi et al. [7,8] have demonstrated the ability of RWS connections to re-classify a connection from partial- to full-strength while still leveraging the full benefit of the ductile Vierendeel mechanism. This was due to the reduction of beam web section, resulting in a reduction of beam's capacities, making the web opening behave as a fuse.

Following the numerical validations, a further parametric investigation was conducted for selected parameters (Table 2) to ensure a well-informed assessment of ductility, energy dissipation and equivalent viscous damping (EVD) coefficient of RWS connections. A total of 504 RWS (single- and double-sided) connections and 6 solid webbed-beam connections counterparts were assessed, and both bare steel and composite connections were considered. The composite connections are divided into absence and presence of composite interactions between

Table 1
Summary of validated tested specimens.

Specimen	RWS	Composite interaction*	Studs	Connection arrangement
Solid connection* *	No	No	Bolted	single-sided $\frac{M_{c.Rd}}{M_{pl.a.Rd}} = 1$
RWS-L-retrofit* *	$d_o = 0.8h$ $S_o = 1h$			
RWS-L* *	$d_o = 0.8h$ $S_o = 0.8h$			
RWS-H* *		Yes		
FI-SU* **	No	No	Welded	double-sided $\frac{M_{c.Rd}}{M_{pl.a.Rd}} = 1.15$
BSF* **		Bare steel		

Note: $M_{c.Rd}$= connection bending capacity. $M_{pl.a.Rd}$= plastic bending capacity of unperforated steel beam section.
*The presence of composite action interaction over the protected zone.
**Reference [7].
* **Reference [41].

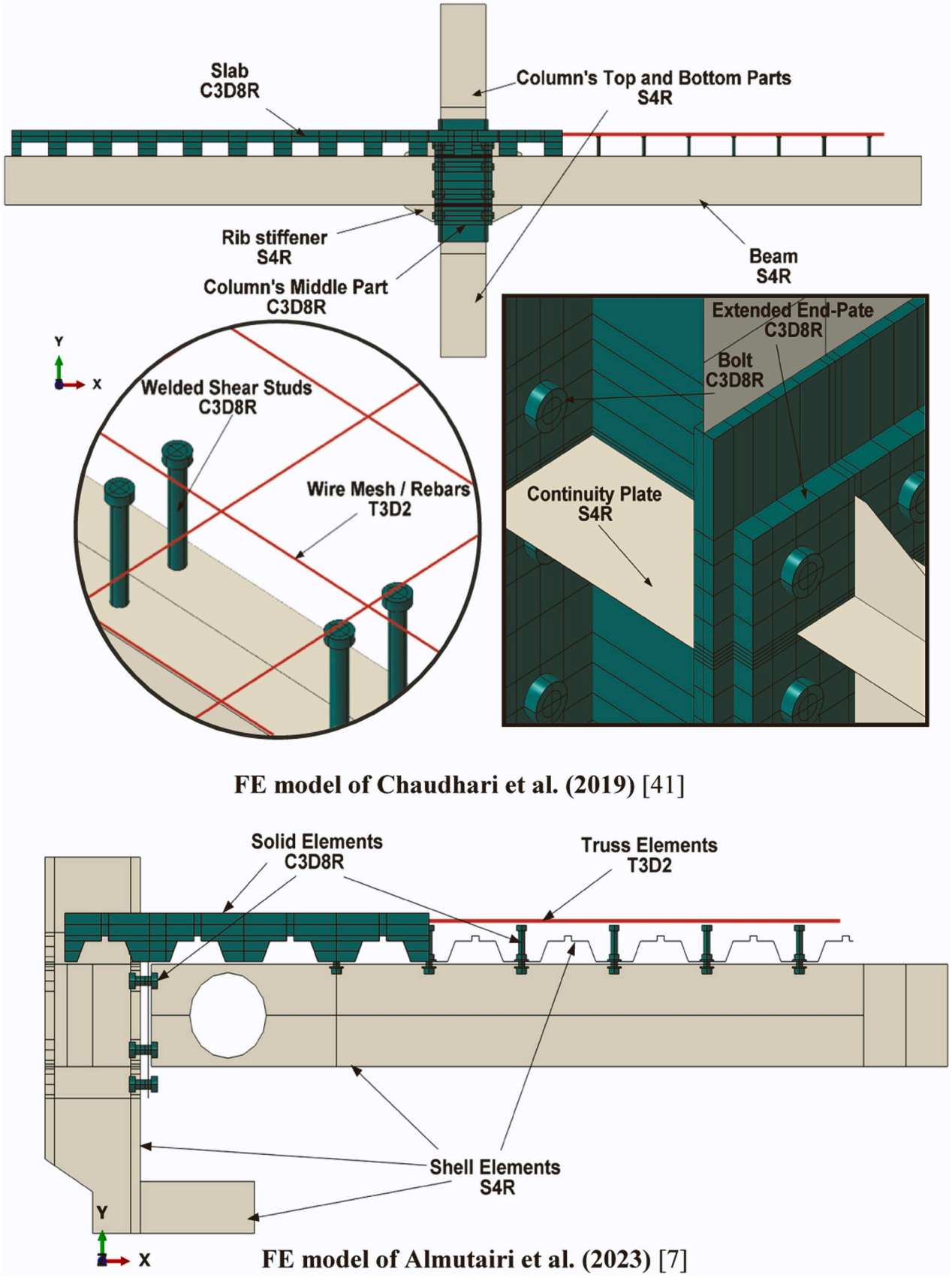

Fig. 5. Selected element types for FE model.

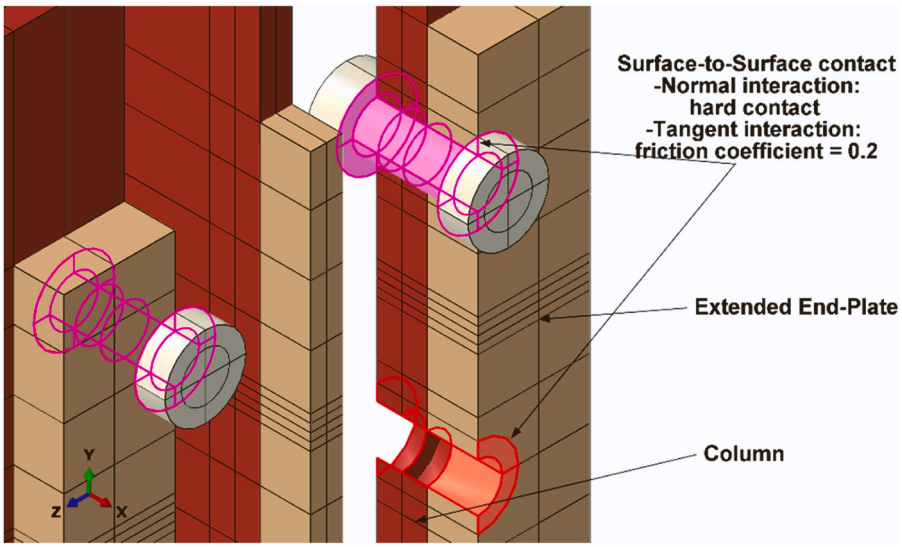

Fig. 6. Normal and tangent interactions with friction between bolts and steel components.

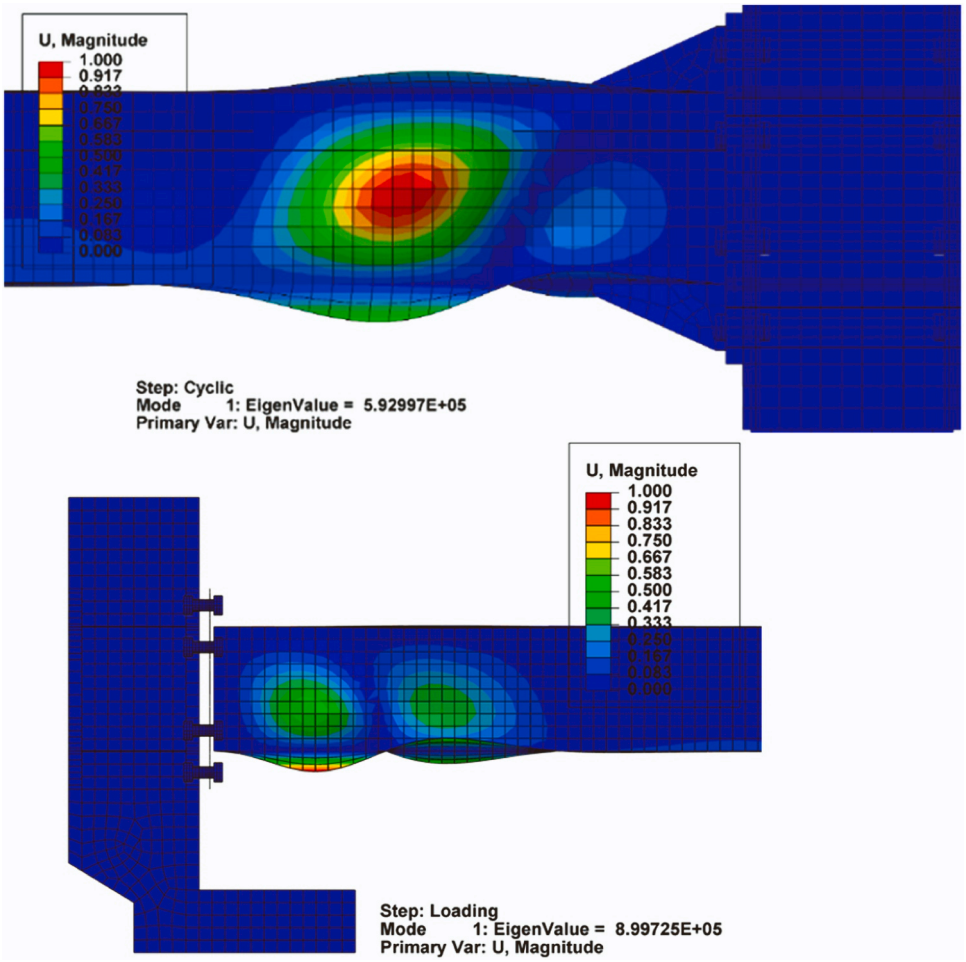

Fig. 7. First shape of Eigenmode.

composite slabs and beams (i.e., high composite action: *placing bolted/welded shear studs,* and low composite action: *no bolted/welded shear studs* above the protected zone). Welded and bolted shear studs were used in double-sided connections and single-sided connections, respectively. It is worth noting that the steel sections used in this parametric study remained consistent with those used in the experimental tests, the UK sections [7] and New Zealand sections [41], shown in Fig. 4.

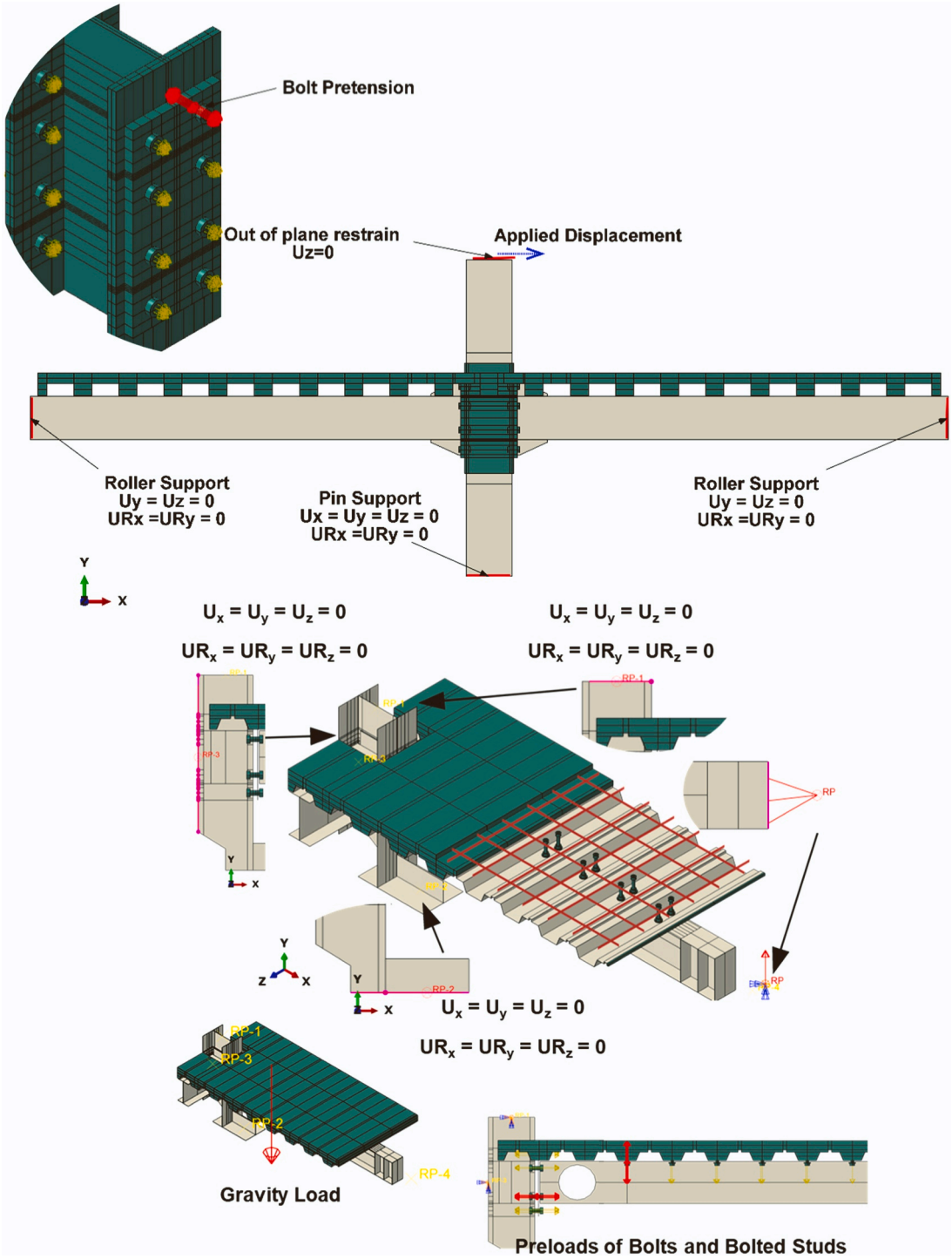

Fig. 8. Boundary condition and bolts pretensions.

4.3. Parametric results

The main objective of this section is to examine the effects of introducing web opening in both partial- and full-strength solid webbed-beam connections. The discussion focuses on assessing the four key factors namely i) the location – from the connection (i.e., the column face) to the centreline of the perforation, ii) the size of web opening, iii) the capacity design ratio, and iv) the presence/absence of composite action. These factors were selected for assessment owing to their crucial impacts on ductility, energy dissipation, and EVD as it was reported in the literature. It is worth noting that for a fair comparison with single-sided connections, the response of the right beam's connection in the double-sided joint was used in this study. The box-and-whiskers plots in this paper, provide a clear visual comparison of ductility, energy dissipation, and EVD for the studied FE models. The models are categorised based on web opening diameter ($50\boldsymbol{d_o}$ to $80\boldsymbol{d_o}$) variations. This visual representation facilitates the evaluation of how the web opening location (end distance, $\boldsymbol{S_o}$) affects the ductility, energy dissipation, and EVD. Furthermore, the plots incorporate the presence and absence of composite action over the web opening as well as bare-steel connection, enabling a thorough assessment of this factor's impact.

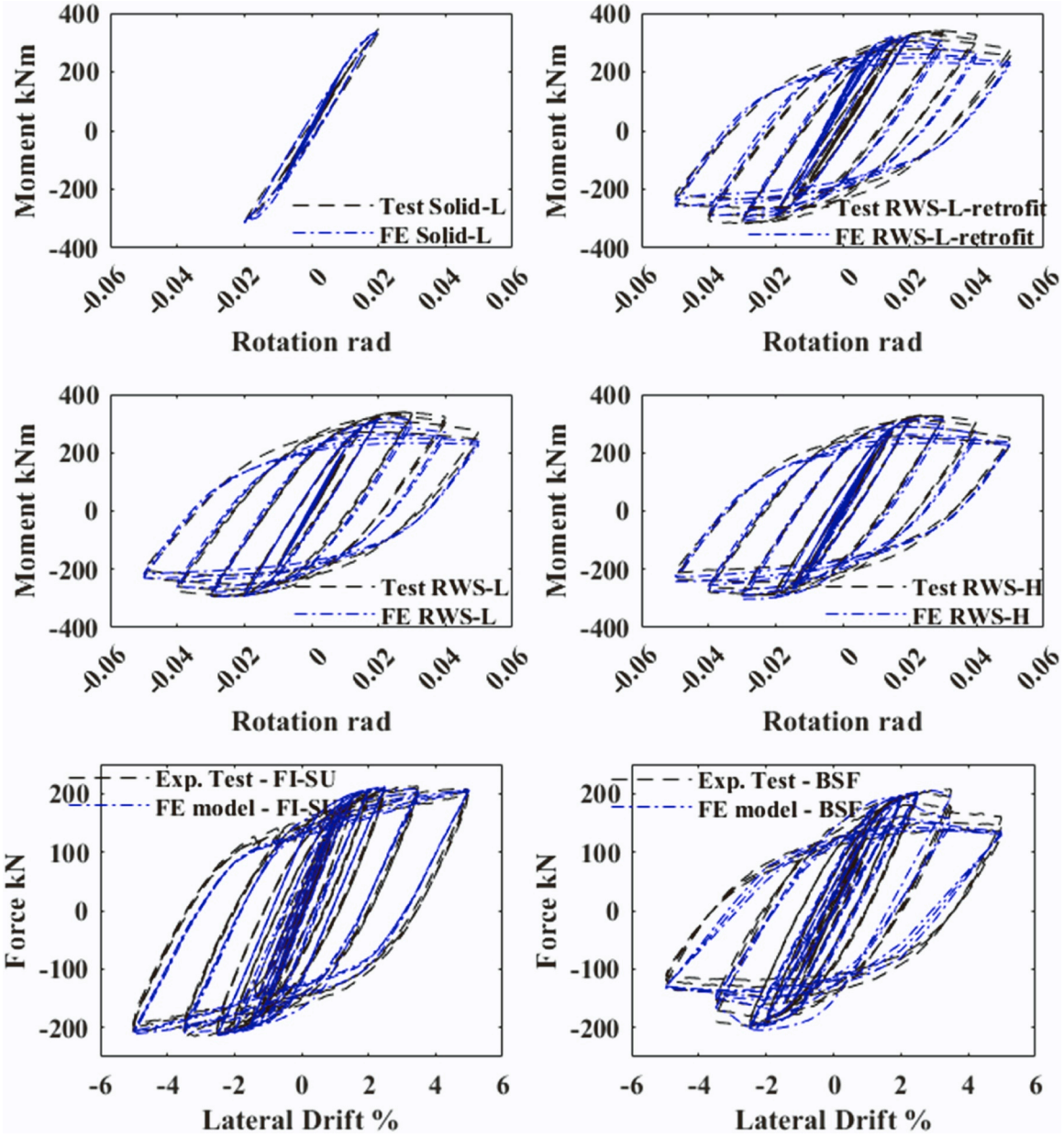

Fig. 9. Benchmarking of the FEM hysteretic responses.

4.3.1. Ductility

One of the key response characteristics to examine the robustness of MRFs under seismic loads is the rotational ductility of the connections. The ductility needs to be present in designated structural components for safe transfer and redistribution of loads within MRFs. It is quantified as the ratio of the ultimate rotation to yield rotation ($\boldsymbol{\theta_u/\theta_y}$). It is worth emphasising that the single-sided and double-sided RWS connections were designed based on equal-strength ($\boldsymbol{M_{c,Rd}/M_{pl,a,Rd} = 1}$) and full-strength ($\boldsymbol{M_{c,Rd}/M_{pl,a,Rd} = 1.15}$) connections with a solid webbed-beam, respectively.

The location of the web opening has less effect on the ductility among the other key factors. Generally, as the location of the web opening moves farther from the connection, both the sagging and hogging ductility ratios decrease. This finding has been established in the literature [21,35–37], where it is shown that the effects of RWS diminish as the end distance ($\boldsymbol{S_o}$) increases. In other words, the formation of a Vierendeel mechanism directly enhances ductility.

The web opening size is the factor that has the most significant consequences, when considered in combination with other factors, in affecting the ductility, as shown Figs. 12 and 13. This is mainly attributed to the Tee-section depth that directly triggers the yielding of the perforated section as shown in Fig. 14. The earlier the Tee-section yields, the higher is the ductility, provided that ultimate rotations remain equal or constant among other RWS connections. This is because of the mathematical formulation of ductility ($\boldsymbol{\theta_u/\theta_y}$) indicates that lower yield rotation leads to higher ductility.

Fig. 14 also demonstrates the combined effects of the web opening size with the presence or absence of composite interaction. The location of the extra row of bolts/welded shear studs has also, an effect on the onset of yielding in the top Tee-section. The critical location of shear studs is at the centreline of the "*circular*" web opening due to the smaller Tee-section depth. Such combination effects can be seen in Fig. 12. Although the number of numerical models using RWS connections with $50d_o$ amounted to 15, the ductility range is narrow (i.e., the maximum and minimum values were close). Conversely, the ductility range of RWS connections with $80d_o$ is wider, despite the small number of numerical

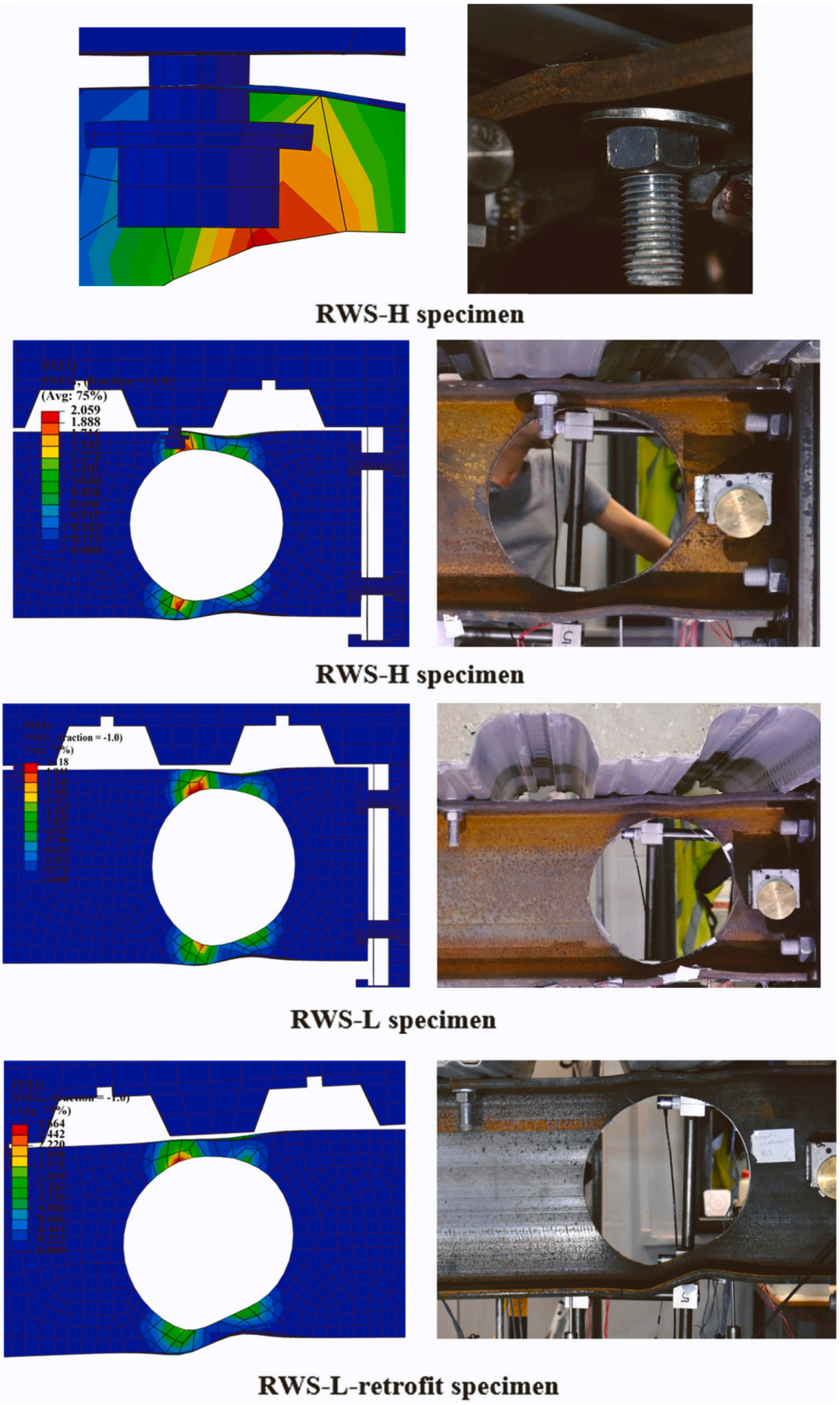

Fig. 10. Comparison between FE models and tested specimens [7] (without rendering the thickness of shell element).

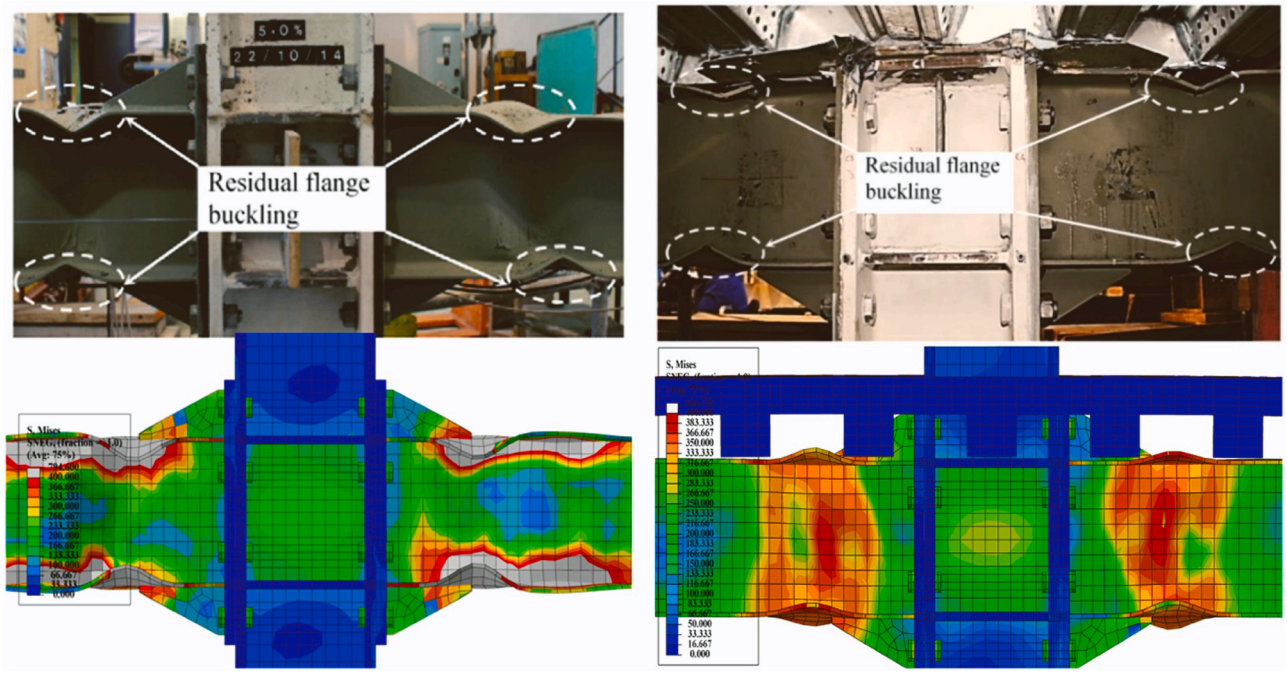

Fig. 11. Comparison of local buckling between experimental tests and FE model (with the rendering of the thickness).

Table 2
Summary of parameters.

1) Diameter d_o			2) End distance S_o		3) The interaction between composite action	
%	mm	Number of models	%	mm	Type	Number of models
50 %	155	15 x 2	50 %	155	High interaction	168
55 %	171	14 x 2	55 %	171	Low interaction	168
60 %	186	13 x 2	60 %	186	bare steel (no interaction)	168
65 %	202	12 x 2	65 %	202		
70 %	217	11 x 2	70 %	217		
75 %	233	10 x 2	75 %	233		
80 %	248	9 x 2	80 %	248		
			85 %	264		
			90 %	279		
			95 %	295		
			100 %	310		
			105 %	326		
			110 %	341		
			115 %	357		
			120 %	372		

Note: High interaction = there are bolted/welded shear studs over the web opening. Low interaction = no bolted/welded shear studs over the web opening. Without composite slab = steel RWS connection. $\boldsymbol{h}$ = beam height; $80\boldsymbol{d_o}$= means the opening diameter equals 80 % of $\boldsymbol{h}$; $80S_o$ = *means the end distance equal 80 % of* $\boldsymbol{h}$.

models that complied with SCI-P355 guidance [26] as shown in Table 2. This was more pronounced with the presence of composite action as compared to those without composite interactions (Fig. 12). This observation applies to single-sided RWS connections (equal-strength), but not to double-sided RWS connections (full-strength) due to the capacity design ratio, as shown in Fig. 13.

Given that, the capacity design ratio could reduce the effectiveness of large web opening, especially with the presence of composite action as shown in Fig. 13, this is mainly attributed to the fact that the RWS connections were designed based on the full strength of the solid webbed-beam connection. For such full-strength connections, deformation primarily occurs in the beam itself, as the connection's capacity exceeds that of the connected unperforated steel beam. In other words, when the web opening is introduced, the steel beam becomes weaker, leading to an earlier yielding. Additionally, the arrangement of the joint (double-sided) and applied cyclic loads on the column tip caused early deformations of Tee-sections due to the high forces acting on the beams from the column.

The behaviour of RWS connection whether designed based on partial- or full-strength solid webbed-beam connections can be more accurately predicted by eliminating the composite slab-beam interaction over the protected zone, as depicted in Figs. 12 and 13. This conclusion is drawn from the observation that the trends of RWS connections in this parametric investigation are similar to those of bare steel RWS connections under both sagging and hogging moments. These findings align with Almutairi et al. [7,8] regarding the superior cyclic behaviour of RWS connections with an absence of composite action to avoid high strain demand on the beam bottom flange, as well as cracking and crushing of the concrete slab, without jeopardising the 'strong column-weak beam' concept, following the requirements of [28,30].

It can be concluded that, for single-sided RWS connections that are designed based on partial-strength solid webbed-beam connection, the sagging and hogging ductility marginally improves when the d_o/S_o ratio equals 1 for diameter equal $0.5h$ and $0.55h$. The improvement in ductility becomes more pronounced with web opening diameters equal to $0.60h$ and $0.65h$ when the d_o/S_o ratio ranges between 0.92 to 1.0 and 0.81 to 1.0, respectively. The range of d_o/S_o ratio broadens for diameter equal $0.70h$, $0.75h$ and $0.8h$, and they were significantly influenced by the presence of composite action over the web opening. For these diameters, the ideal d_o/S_o ratios range between approximately 0.7 to 1.0.

For double-sided RWS connections that are designed based on full-strength solid webbed-beam connection, the ductility alone cannot capture the overall response of the RWS connection. The energy dissipation and EVD must also be considered when introducing web openings into full-strength solid webbed-beam connections.

4.3.2. Energy dissipation and equivalent viscous damping

Although ductility is an important indicator in seismic design, it alone cannot capture the overall hysteretic response of the structure. For instance, the pinching phenomenon is well-represented by the area of

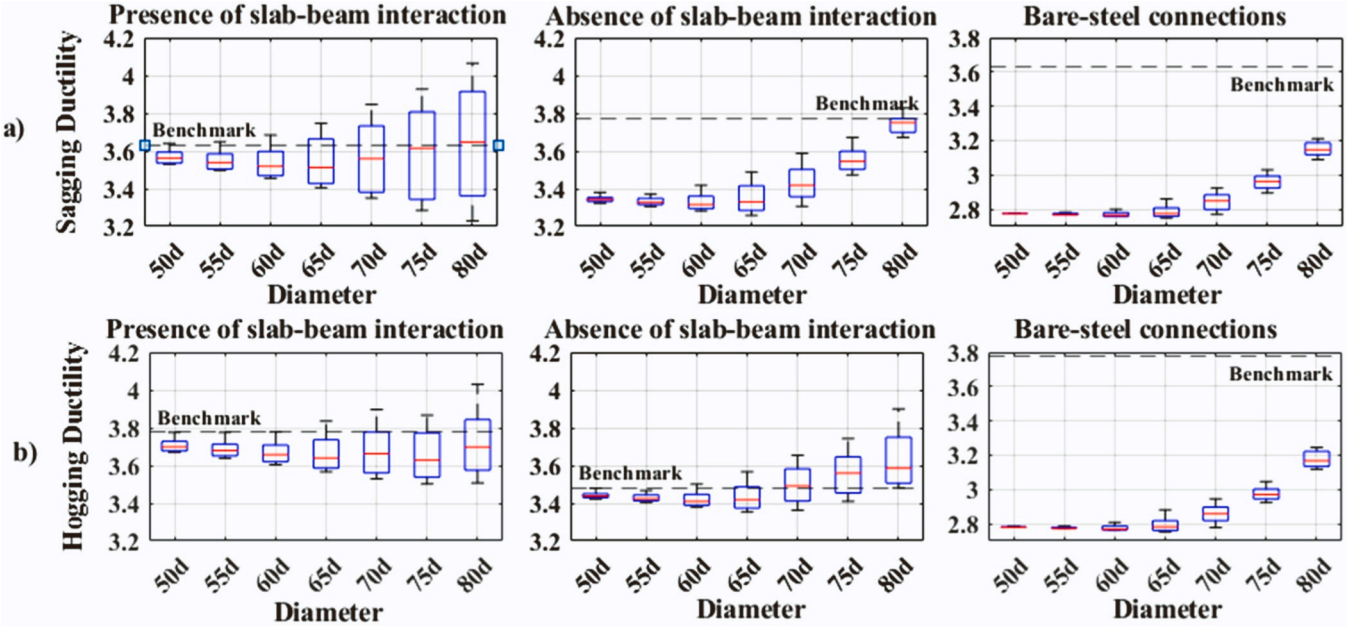

Fig. 12. Ductility of single-sided connections (based on equal-strength solid webbed-beam connection), the benchmark = the connection with solid webbed-beam (without web opening).

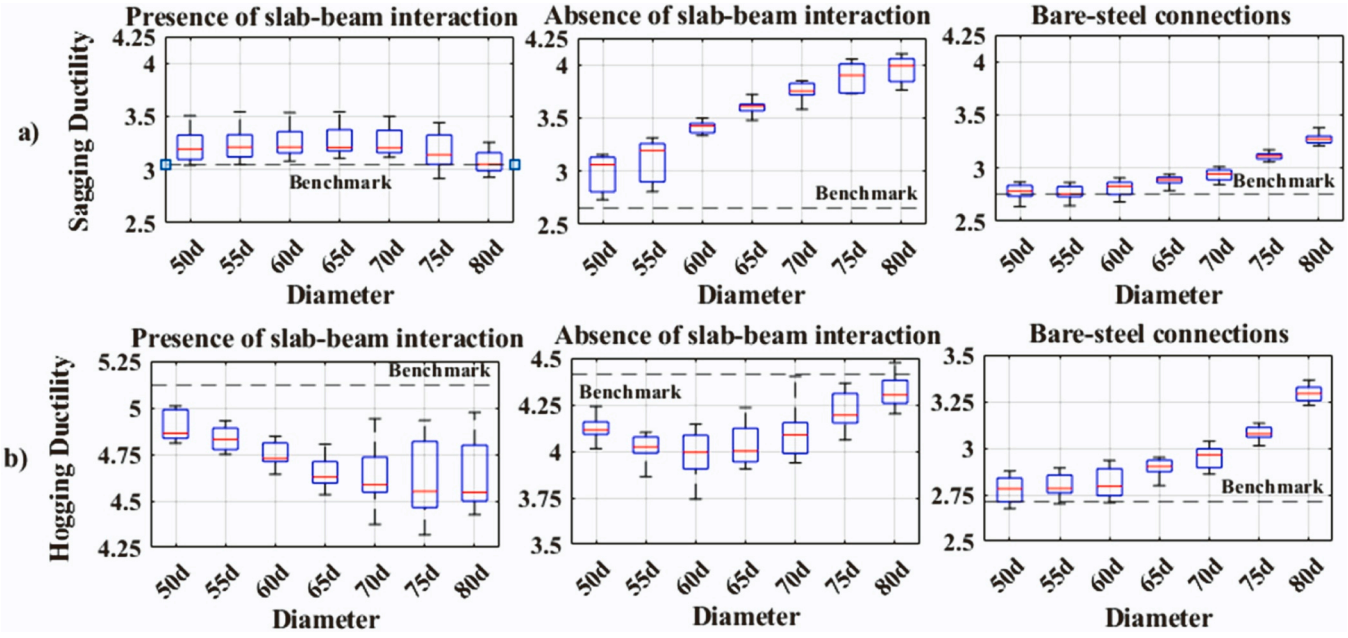

Fig. 13. Ductility of double-sided connections (based on full-strength solid webbed-beam connection), the benchmark = the connection with solid webbed-beam (without web opening).

the hysteresis loops which depicts the amount of seismic energy dissipated in each cycle. Fig. 12 shows that in some cases the RWS connections with smaller web openings could achieve higher ductility. In these cases, the bending of the extended end-plate acted as one of the dissipative elements, leading to a pinching mechanism and a significant reduction in the total amount of dissipated seismic energy, as shown in Fig. 15. This was well captured in this parametric study, as shown in Figs. 12b and 16 for single-sided connections (equal-strength). The web openings with small sizes have higher hogging ductility on average and lower dissipated energy compared to the large size of web openings. However, this is not the case for the double-sided RWS connections.

Double-sided connections were designed based on a full-strength connection with a solid webbed beam, so they were intended to have the beam serve as the primary dissipative element. Thus, any web opening, regardless of size, would serve as a predetermined location for plasticity. For RWS connections with the presence of composite action, an increase of 15 % of the connection's moment capacity led to an average difference of 21 % in dissipated energy in favour of the web opening with $50d_o$ in comparison with $80d_o$. These findings are in line with the findings of Shaheen et al. [11] and Almutairi et al. [7,8] which advocate for the use of small to medium web opening sizes when a high capacity design ratio was considered. When employing a high-capacity design ratio, it is recommended to use small to medium web opening sizes, and the opposite when lower-capacity design ratios are employed.

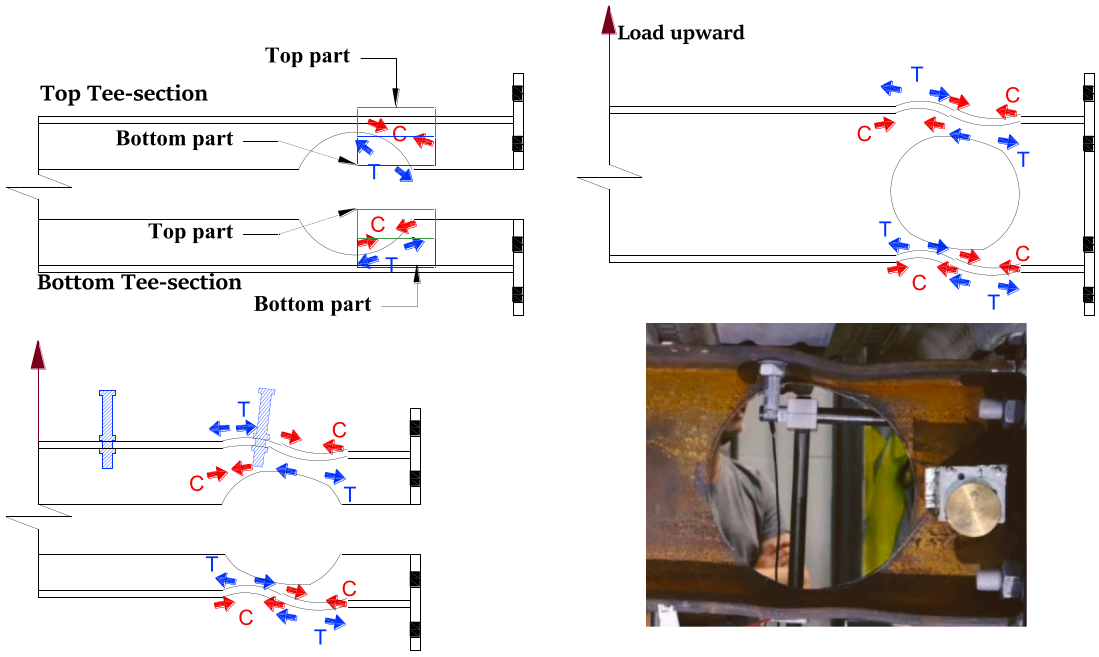

Fig. 14. Illustration of the behaviour of Tee-sections [7].

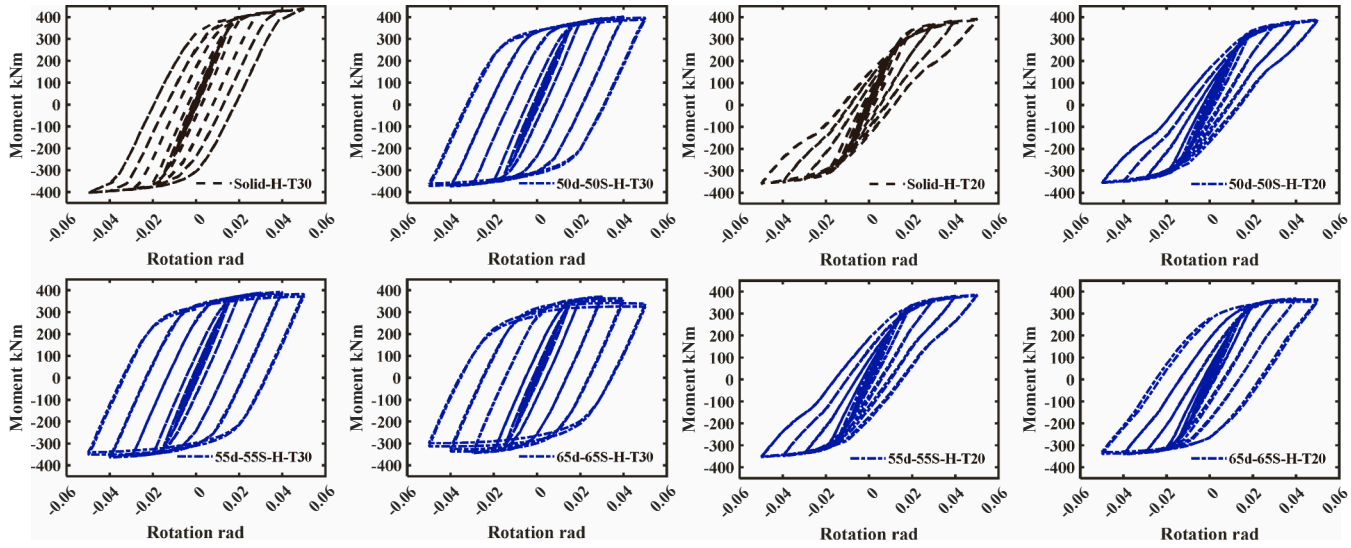

a) Thickness of end-plate = 30 mm $\frac{M_{j,Rd}}{M_{pl,a,Rd}} = 1.06$ (full-strength connection).

b) Thickness of end-plate = 20 mm $\frac{M_{j,Rd}}{M_{pl,a,Rd}} = 1$ (equal/partial-strength connection).

Fig. 15. Capacity ratio comparison of two connections with composite action over the web opening.

Overall, double-sided RWS connections with $50d_o$ and $55d_o$ demonstrate impressive responses, offering both superior energy dissipation and competitive ductility compared to other designs, including the stiffened BEEP (FI-SU) with a value of 109.5 kNm.rad. The findings suggest that RWS connections work more effectively when designed based on partial/equal-strength solid webbed-beam connection. This originates from a predictable hysteretic response.

Another important indicator to evaluate the energy dissipating capacity of the connections is an EVD ratio (ξ_{eq}) [48]. EVD quantifies a system's capacity for energy dissipation with higher values as it dissipates more energy, reduces dynamic response, and mitigates resonance. Conversely, lower EVD allows for quicker response but may lead to excessive vibrations and heightened vulnerability to resonance. The energy dissipation is examined in terms of EVD and defined as:

$$\xi_{eq} = \frac{1}{2\pi} \frac{S_{ABC} + S_{CDA}}{S_{ODA} + S_{OBF}}$$

The energy depicted by $S_{ABC} + S_{CDA}$ is the energy dissipated at the expected rotation as shown by the shaded region in Fig. 17. Similarly, $S_{ODA} + S_{OBF}$ indicates the total strain energy at the expected rotation highlighted by the area with double shading in Fig. 17. Furthermore, points B and D represent the peak positive and negative moment capacities within a hysteresis loop, respectively. The EVD coefficients at 0.04 rad for all models are shown in Fig. 18. At the rotation of 0.04 rad, the magnitudes of EVD generally were above 30 % which indicates good energy dissipation capacity and seismic response of RWS connections.

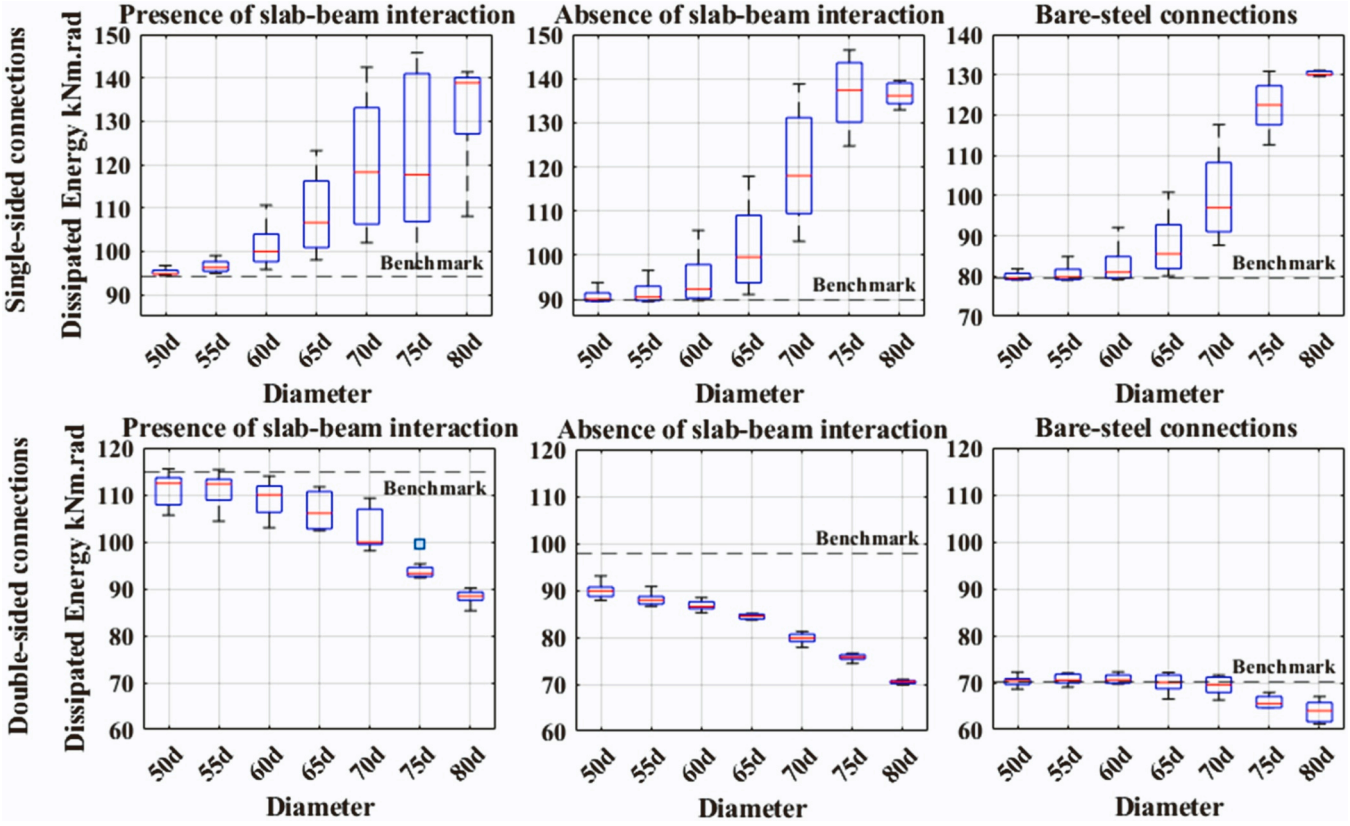

Fig. 16. Energy dissipation, the benchmark = the connection with solid webbed-beam (without web opening).

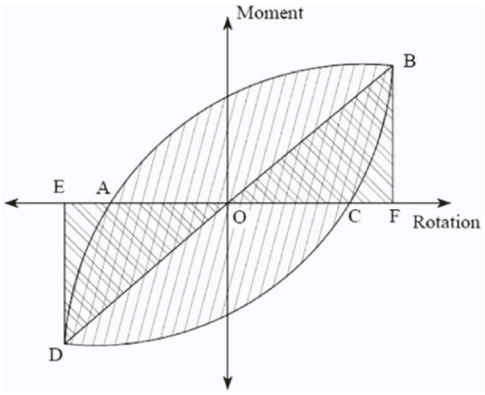

Fig. 17. Basis to calculate the equivalent viscous damping coefficient.

These also imply that the RWS connection has not experienced brittle or sudden failures, likely maintaining its integrity, which is crucial for the stability of the structure and safety immediately after the earthquake.

5. Capacity assessment

5.1. RWS database assembly

The assembled RWS connections database consists of 13 experimental and FE studies, excluding this study. This database covers both bare steel and composite RWS connections as well as benchmarked solid webbed-beam connections. It contains data on both welded and BEEP (3 rows and 4 rows of bolts) connections. Additionally, the database captures only a single circular web opening. In total, there are 251 specimens and FE models for 247 RWS connections, in addition to their benchmarked 14 solid webbed-beam connections counterparts. The database accounts for different types of test setups, namely, cantilever, cruciform and frame arrangements, with load and/or displacement applied at the beam, or the column ends. Although this is a comprehensive RWS connections' database, a few experimental and FE programmes were excluded from the current list due to scarce test and FE details. A summary breakdown of the collected RWS database is presented in Table 3 and Table 4.

5.2. Deduced response parameters of the collected RWS database

The response parameters of the collected RWS database were deduced through two methods, as mentioned previously in Section 3. The first method involved manually extracting numerical values from moment-rotation (**M-θ**) curves based on the IMK model, as illustrated in Fig. 3. The second method extracted data from tabulated results found in research papers within the literature. Both experimental and numerical results were normalised concerning the nominal plastic moment capacity of the steel solid webbed-beam sections.

For a fair comparison, the energy dissipation and EVD for both sagging and hogging moments were calculated. These calculations utilised key response parameters (normalised moments and rotations) as described in Section 3 and depicted in Fig. 19. Both tri-linear and bi-linear skeleton **M-θ** curves based on the IMK model [42] were employed. The tri-linear skeleton **M-θ** curve is detailed in Section 3. The bi-linear skeleton **M-θ** curve was used for two specific cases. The first case applied when the connection did not undergo strength degradation, thus equating $\boldsymbol{M_u}$ with $\boldsymbol{M_m}$ and $\boldsymbol{\theta_u}$ with $\boldsymbol{\theta_m}$. The second case was used when the corresponding rotation or/and moment data was unavailable in the tabulated results from literature. For instance, if $\boldsymbol{M_u}$ and $\boldsymbol{\theta_m}$ were not provided while $\boldsymbol{M_m}$ and $\boldsymbol{\theta_u}$ were available, then bi-linear skeleton **M-θ** curve was used.

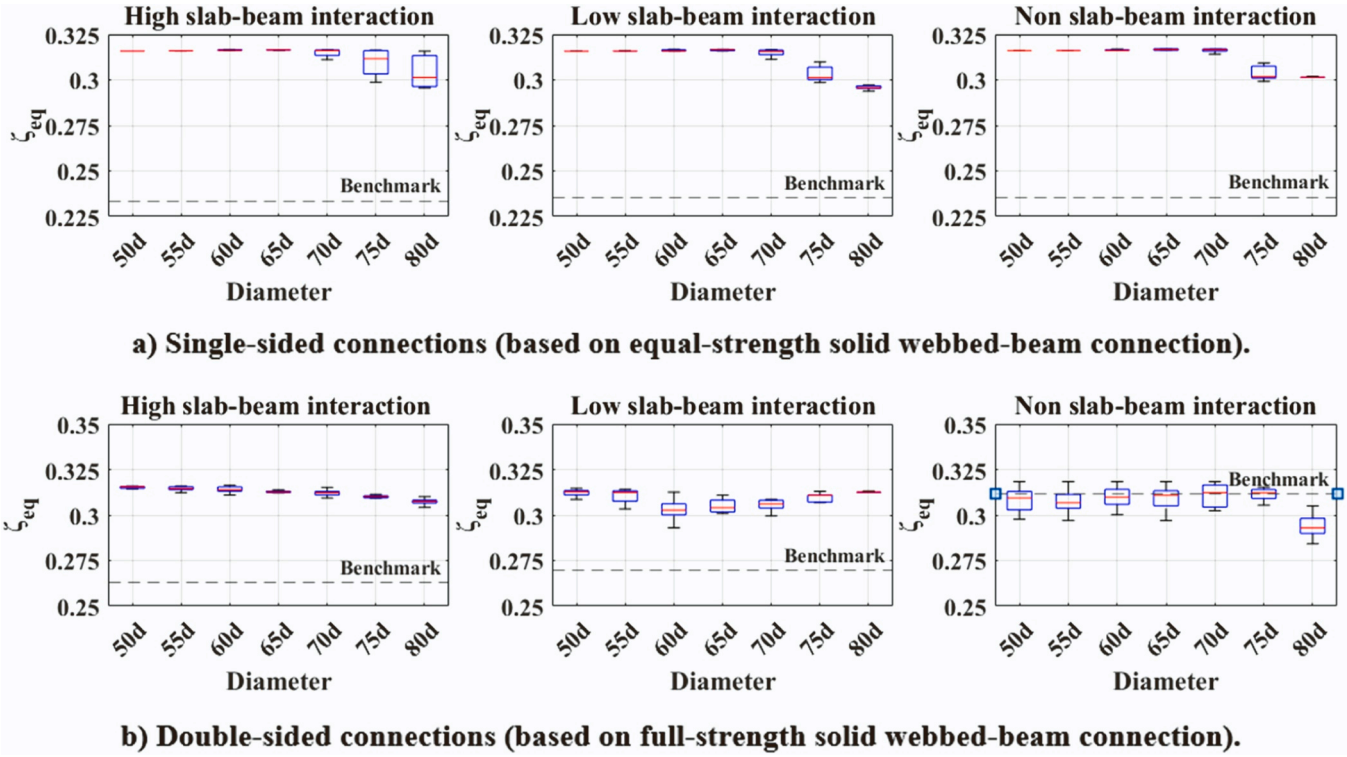

Fig. 18. Equivalent viscous damping coefficient at 0.04 rad, the benchmark = the connection with solid webbed-beam (without web opening).

Table 3
Summary breakdown of the collected RWS database.

Reference	Study	Joint	Connection	# of specimens	Slab
Guo et al.[49]	FE	Frame	Welded	6	No
Li et al. [50]	Exp	Cantilever	Welded	3	No
Tsavdaridis et al. [36]	FE	Cantilever	Welded	9	No
Tsavdaridis and Papadopoulos [37]	FE	Cantilever	BEEP-3-R	1	No
Shin et al. [13]	Exp	Frame	WUF-B	2	No
Erfani and Akrami [51]	FE	Cantilever	Welded	1	No
Shaheen et al. [11]	FE	Cantilever	PN	12	Yes
Zhang et al. [52]	Exp	Cantilever	Welded	1	No
	FE			1	
Boushehri et al. [35]	FE	Cantilever	Welded	144	No
Nazaralizadeh et al. [53]	FE	Cantilever	BEEP-4-R	1	No
Xu et al. [54]	Exp	Cantilever	Welded	5	No
Almutairi et al. [8]	FE	Cruciform	BEEP-4-R	45	Yes

Note: # = number. FE = Finite element analysis. Exp. experimental test. BEEP-3-R and 4-R = bolted extended end-plate with 3 rows and 4 rows, respectively. WUF-B = welded unreinforced flange-bolted web. PN = pre-Northridge.

5.3. Observed trends in the collected RWS database

The collected database reveals a range of beam, column, connection types and capacity design ratios. An inconsistency in capacity design ratios was observed. The capacity design is a key requirement in controlling the plastic response of beam-to-column joints by managing the connecting components' capacities. With this objective in mind, employing the capacity design in RWS connections is critical since the reduction in shear capacity is particularly undesirable in seismic areas because it deteriorates more rapidly than its moment capacity. However, the concept of RWS connection, which relies on the Vierendeel mechanism, is only effective in areas of high shear. The Vierendeel mechanism is a shear action that requires a large opening and an ideal end distance to be triggered. Otherwise, a non-ductile failure characterised by tearing and out-of-plane buckling may ensue. Chung et al. noted that both shear failure and the Vierendeel mechanism can occur concurrently in the vicinity of the web opening [16,17]. Therefore, attention should be paid not only to the size and location of the web opening, which have been the focus of previous studies in the literature, but also to the capacity design ratio between the connected components. This is to ensure that the beam's shear capacity is not excessively compromised by the incorporation of the RWS (reduced web section). To this end, a balanced contribution (capacity design) of a panel zone, end-plate and/or column flange, with the connected bare steel solid webbed-beam, is preferable in an RWS connection. This promotes a Vierendeel (ductile) mechanism to become the dominant failure rather than simple shear failure at the web opening, which may cause instability after an earthquake. This is consistent with prior observations of the studies of Almutairi et al. [7,8] regarding the importance of capacity design ratios. These findings are verified by the review of the collected RWS database, in which, the web opening size should be decreased along with the capacity design ratio increase.

Having thoroughly examined the collected RWS database, the above conclusions are verified. Figs. 20 and 21 display the trends in the RWS database between energy dissipation, EVD, and ductility concerning the capacity design ratio. It can be seen that an increase in the capacity design ratio leads to a decrease in energy dissipation, EVD, and ductility, regardless of the connection type. Fig. 21 depicts the decrease in sagging ductility of identical connections with an increase in web opening size with a high capacity design ratio, as employed in the study of Shaheen et al. [11]. In contrast, Almutairi et al. [8] observed an increase in sagging ductility of identical connections with a decrease in web opening size when accompanied by an equal/partial capacity design ratio. Figs. 20 and 21 highlight the importance of capacity design ratios in RWS connections compared to solid webbed-beam connections. A capacity design ratio larger than 1.5, is preferable with a solid webbed-beam connection to account for steel hardening and to prevent fracture, as suggested by Elkady and Lignos [56]. This is not applied to

Table 4
Summary of capacity design breakdown of the collected RWS database.

Ref.	Connection	Column Section $M_{pl.col} = W_{pl.y.c}$ $f_{y.c}$	Beam Section $M_{pl.b} = W_{pl.y.b}$ $f_{y.b}$	Connection capacity $M_{c.Rd}$ using Component method EC3-1-8 [55]	Capacity design ratio
[49]	Welded	H500 × 350 × 14 × 18 911	H600 × 250 × 10 × 14 710	NA	1.28
[50]	Welded	H450 × 300 × 12 × 16 613	H400 × 200 × 8 × 12 285	NA	2.15
[36]	Welded	HEB 300 570	HEA 240 227	NA	2.51
[37] [37]	BEEP-3-R	HEB 160 97	IPE 300 173	87	0.50
[13]	WUF-B	W14X145 1763	W12X50 439	NA	4.02
[51]	Welded	HB500x200x10x16 735	HB414x405x18x28 1735	NA	0.42
[11]	PN	HB428x407x20x35 2051	HB700x300x13x24 1490	NA	1.38
[52]	Welded	HW250x250x9x14 220	HN300x150x6.5x9 123	NA	1.79
[35]	Welded	HEB 300, 450, 500, 600 663, 1414, 1709, 2599	IPE 330, 450, 500, 600 285, 604, 779, 1247	NA	2.32, 2.34, 2.19, 2.08
[53]	BEEP-4-R	HEB 200 154	IPE 270 116	95	0.82
[10]	BEEP-3-R	UC 203 x 203 x 71 284	UB 305 x 127 x 48 252	157	0.62
[54]	Welded	HW250x250x9x14 220	HN300x150x6.5x9 123	NA	1.79
[8]	BEEP-4-R	HEB 320 765	IPE 300 224	216	0.96

Note: M_{pl}= moment capacity of bare steel solid webbed-beam section. [kNm]. $W_{pl.y}$ = plastic section modulus. f_y= yield strength. Subscript col, b and c = column, beam and connection, respectively. BEEP-3-R and 4-R = bolted extended end-plate with 3 rows and 4 rows, respectively. WUF-B = welded unreinforced flange-bolted web. PN = pre-Northridge.

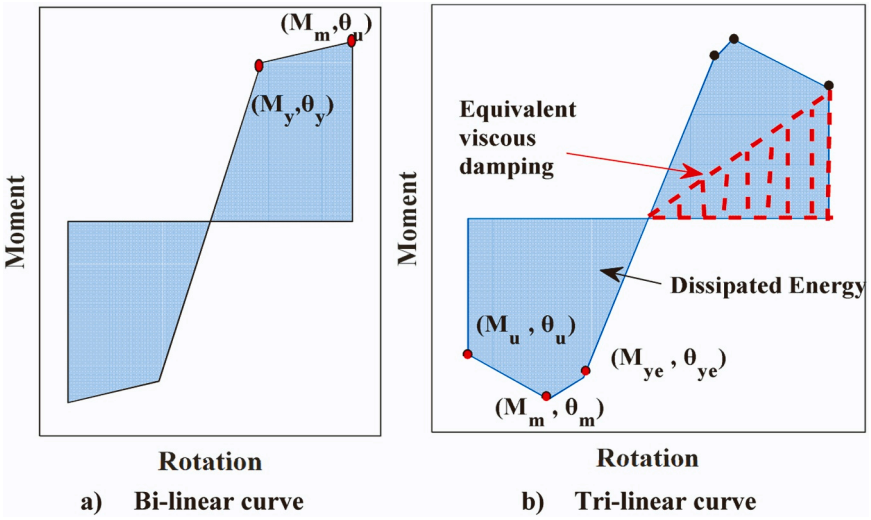

Fig. 19. Skeleton moment-rotation curves used for the collected RWS database.

RWS connections. However, the high ductility found in RWS connections with a high capacity design ratio (larger than 1.5), can be attributed to two factors. The first is the early yielding of Tee-sections, which leads to higher ductility. The second is the exclusion of the composite slab from testing, which would have resulted in a higher ultimate rotation and, consequently, higher ductility.

6. Detailing recommendations

Different design methodologies for RWS connections have been proposed in the literature [21,34,35,52,57–59] based on the current design guidelines for perforated beams in both the UK and the US [26,27,60] as well as on the design process for RBS connection outlined in AISC-385 [28]. Despite the consideration of the 'strong column-weak beam' concept, all proposed design methodologies for RWS connections have not yet addressed the capacity design ratio between the connected components. The 'strong column-weak beam' and capacity design concepts are similar in that they aim to control how structures respond to earthquakes. Yet, they approach the design objectives in different ways.

The 'strong column-weak beam' concept is a design rule that is limited to beams and columns. It is intended to prevent column failure by ensuring that plastification forms in beams before it does in columns. This is important since the columns' failure can lead to the progressive

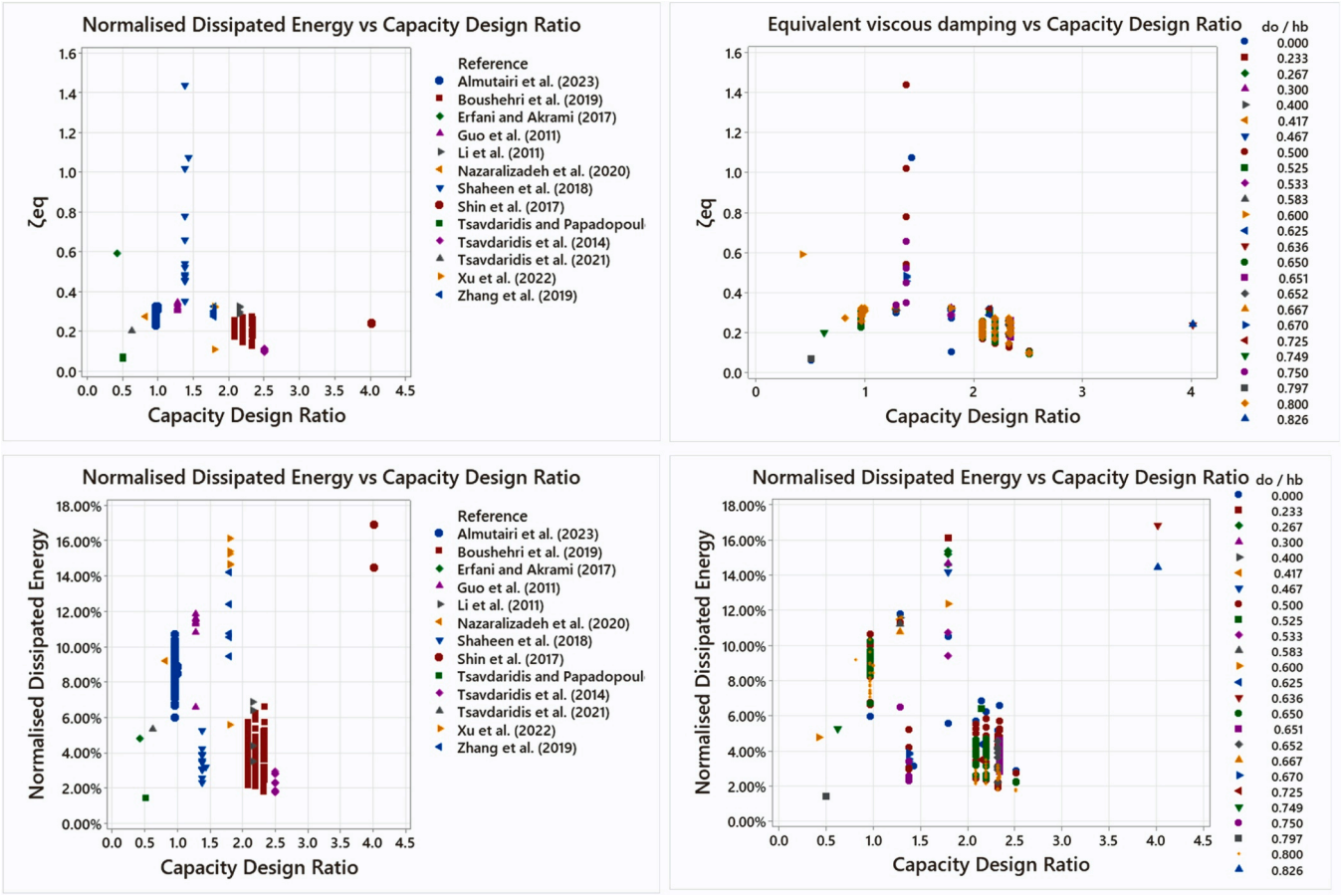

Fig. 20. Energy dissipation and equivalent viscous damping.

collapse of a structure. On the other hand, capacity design is a broader principle aimed at ensuring the proportionate contribution of each component of the joint to the inelastic response of the entire joint. This discrepancy highlights a gap in current design approaches that warrants further investigation and the prequalification of RWS connections with both bolted and welded connections.

Based on the analysis of the collected RWS database and parametric numerical investigation conducted in this study, recommended details for the design of RWS connections are proposed herein. The recommendations pertain to extended end-plate connections with 4 rows of bolts. The proposed details apply to both retrofitting existing structures and designing new ones.

Regarding the retrofit of existing structures, it is noted that steel-concrete composite beams with welded shear studs present challenges. Creating a gap between the concrete slab and the column or removing welded shear studs over the protected zone, would be obstructive and costly. However, such a gap is essential to ensure that no forces are transferred to the column from the concrete slab. This minimises the possibility of slab damage and reduces the strain/stress demand on the column. Therefore, proper consideration of such force transfer mechanisms as stated in Eurocode 8 [30] is required when modelling the joint for retrofit purposes. Table 5 shows the recommended ratios of capacity design, diameter-to-depth (d_o/h_b), and diameter-to-end distance (d_o/S_o) for retrofitting existing structures. The recommendations in Table 5 could serve as a starting point for modelling the joint for retrofitting of existing building.

Specific recommendations for detailing the size and location of web openings in relation to the location of shear studs are critical for both existing and new structures. This is particularly important when composite slab-beam interaction over the protected zone is necessary or unavoidable. Ensuring this can activate the Vierendeel mechanism for small to medium web openings, is significant due to the large depth of the Tee-section at such sizes (Fig. 22). For large web openings, it is preferable to locate them between the studs to avoid a premature crack in the vicinity of web opening.

Although the guidance presented in SCI-P355 [26] was developed for monotonic loads, it has been shown to predict the moment capacity of RWS connections under cyclic loads. It is well-known that the moment capacity of connections under cyclic loads is always lower than that under monotonic loads due to repeated loading and unloading. This repetition causes various mechanisms, such as material low cyclic fatigue, which leads to reduced capacity. This has also been confirmed by the study of Tsavdaridis et al. [21] that the cyclic moment and rotational capacities of the RWS connections were lower than their monotonic counterparts. The guidance outlined in SCI-P355 [26] is derived from the T-section approach (TSA), one that was initially introduced for composite perforated beams [26]. The findings of this study, manifest that the SCI-P355 guidance [26] can be applied to estimate the moment capacity of RWS connections under cyclic loads.

In this study, the effective yield moment (M_{ye}) is used to represent the connection's plastic moment capacity ($M_{c,Rd}$) due to a lack of consensus on its calculation in the existing literature [61]. $M_{c,Rd}$ was employed to assess the bending capacity of the perforated section ($M_{o,Rd}$; $M_{o,Rd,comp}$) in both bare steel and steel-concrete composite connections according to SCI-P355 guidance [26], respectively. Table 6 presents the statistical values indicating the applicability of the SCI-P355 guidance [26] in estimating RWS connections. Table 7 lists the capacity design requirements for RWS connections for new structures. It is worth noting that these requirements follow the capacity design principles of EQUALJOINTS and EQUALJOINTS-Plus [1–3,5,6], with the

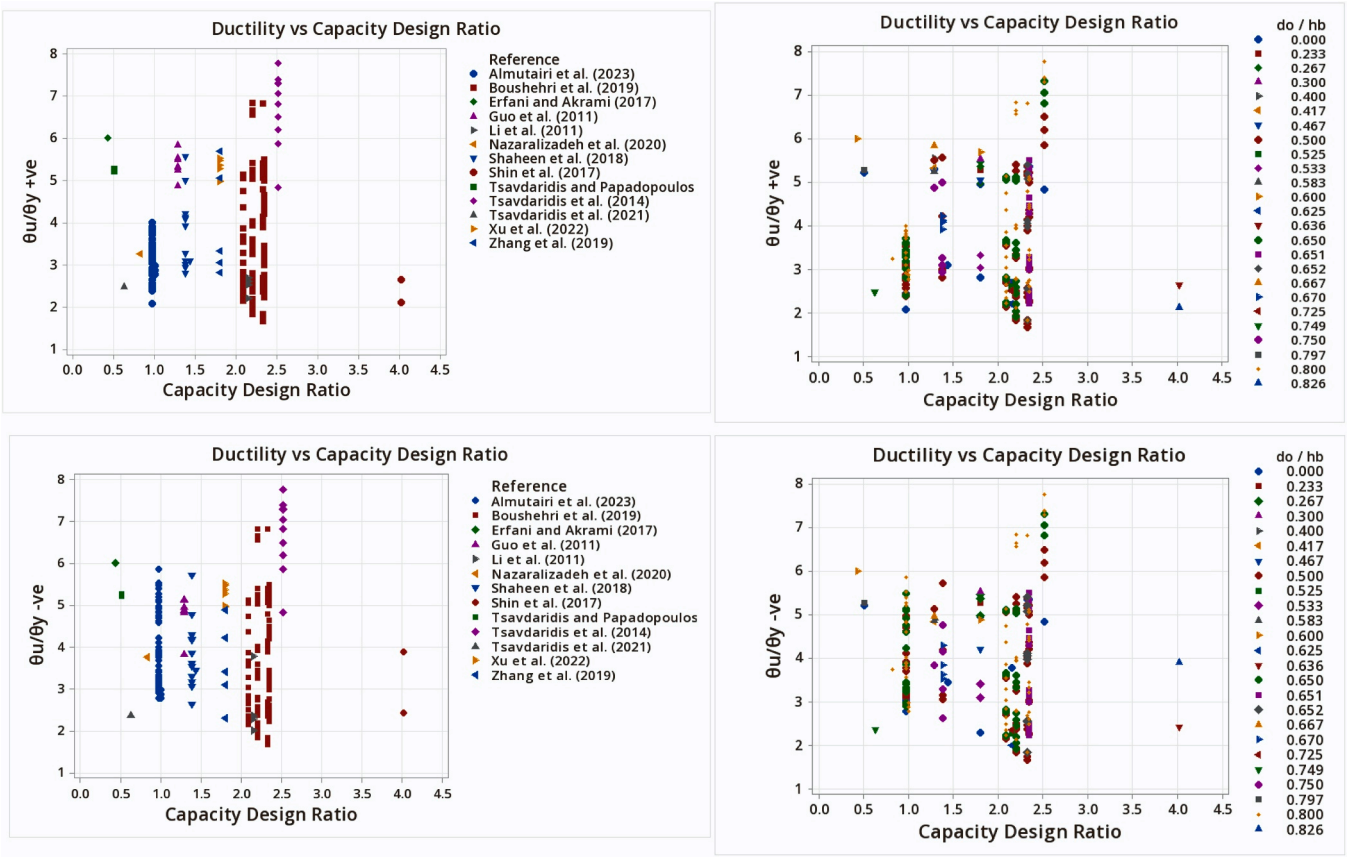

Fig. 21. Ductility for RWS connections.

Table 5
Capacity design requirements for RWS connections for retrofitting existing structures.

Connection's strength category			
Bolted connections	Capacity design ratio		
	Full-strength	Equal-strength	Partial-strength
	$M_{c,Rd} \leq 1.3\ M_{pl,b}$	$M_{c,Rd} = M_{pl,b}$	$M_{c,Rd} \geq 0.8\ M_{pl,b}$
$d_o/h_b =$	0.5 – 0.67	0.7 – 0.8	
$d_o/S_o =$	1	0.7 – 1	

Where $M_{c,Rd}$ = connection bending capacity according to the component method in EC3–1-8 [55]. $M_{pl,b}$ = nominal bending capacity of bare steel solid webbed-beam section. d_o = opening diameter. h_b = steel beam depth. S_o = end distance from column/end-plate face to web opening centreline.

inclusion of recommendations from SCI-P355 guidance [26].

Regarding welded connections, further investigations into the capacity design are required. However, based on the collected RWS

Table 6
Statistical results for the collected RWS database and parametric investigations.

		Sagging	Hogging
$M_{ye}/M_{o,Rd,comp}$	Average	1.1260	-1.0170
	Maximum	1.6426	-0.8196
	Minimum	0.7445	-1.5045
	Standard Deviation	0.1548	0.0891
$M_{ye}/M_{o,Rd}$	Average	1.0618	-1.0582
	Maximum	1.2439	-0.7954
	Minimum	0.7933	-1.2618
	Standard Deviation	0.0635	0.0644

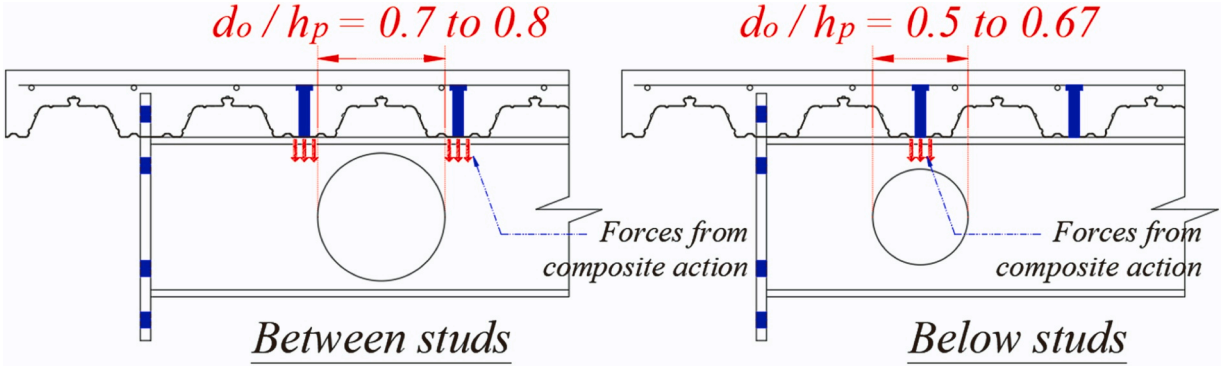

Fig. 22. Diameter-to-depth ratio in relation to shear studs' location.

Table 7
Capacity design requirements for RWS connections for new structures.

•Full-strength: $M_{c,Rd} \geq 1.1 \cdot \gamma_{ov} \cdot (M_{o,Rd,comp} + V_{Ed} \cdot S_o)$
•Equal -strength: $M_{c,Rd} \geq (M_{o,Rd,comp} + V_{Ed} \cdot S_o)$
•Partial -strength: $M_{c,Rd} \geq 0.8 \cdot (M_{o,Rd,comp} + V_{Ed} \cdot S_o)$

Where $M_{c,Rd}$ = connection bending capacity according to the component method in EC3-1-8 [55]. $M_{o,Rd,comp}$= bending capacity of perforated composite beam section according to SCI-P355 guidance[26].). V_{Ed} is the shear force corresponding to the formation of a plastic hinge in the connected beam, S_o = is the end distance between the connection face and the centerline of web opening. γ_{ov} = the overstrength factor = 1.25.
Diameter-to-depth (d_o/h_b), and diameter-to-end distance (d_o/S_o) for retrofitting existing structures are applicable to design RWS connections for new structures.

database, the ideal d_o/S_o ratio for the welded connection is 1.0 for a diameter equal to 0.5h to 0.67h. The capacity design ratio for the welded connection should be $M_{pl,col} \leq 1.3\ M_{pl,b}$.

7. Conclusions

Capacity design is a comprehensive approach that aims at ensuring that each component of a joint contributes proportionately, behaving in a predictable and ductile manner as part of the entire joint. This approach has not been addressed in previous studies of RWS connections. A comprehensive parametric numerical investigation has been performed for single-sided and double-sided steel-concrete composite connections. Subsequently, a database of 13 experimental and FE programmes on RWS connections was collated. It contains data on both welded and bolted RWS connections with a single circular web opening. In total 247 RWS specimens were included, alongside their benchmarked counterparts, for a total of 14 solid webbed-beam connections.

Both the parametric numerical data and the collected RWS database were analysed to assess the impact of capacity design ratio on ductility, energy dissipation, and EVD. The findings indicate that the cyclic response of RWS connections depends on the capacity design ratio between the connected components of the joint/connection. Consideration of the capacity design ratio ensures that a stable inelastic mechanism is governed when the RWS connection is subjected to cyclic loads. This enhances the ductility and energy dissipation of RWS connections through a stable yielding of Tee-sections, thereby capping plasticity to non-ductile components. Lastly, it is concluded that the assessment of RWS connections manifests the critical effects of the location and size of web opening, in relation to shear studs' location on triggering the desirable ductile Vierendeel mechanism.

Author statement

We the undersigned declare that this manuscript is original, has not been published before and is not currently being considered for publication elsewhere. We confirm that the manuscript has been read and approved by all named authors and that there are no other persons who satisfied the criteria for authorship but are not listed. We further confirm that the order of authors listed in the manuscript has been approved by all of us. We understand that the Corresponding Author is the sole contact for the Editorial process. He/she is responsible for communicating with the other authors about progress, submissions of revisions and final approval of proofs.

CRediT authorship contribution statement

Konstantinos Daniel Tsavdaridis: Writing – review & editing, Supervision, Software, Resources, Project administration, Methodology, Investigation, Funding acquisition, Data curation, Conceptualization. **Fahad Falah Almutairi:** Writing – original draft, Visualization, Validation, Formal analysis, Data curation.

Declaration of Competing Interest

The authors declare that they have no known competing financial interests or personal relationships that could have appeared to influence the work reported in this paper.

Data availability

No data was used for the research described in the article.

References

[1] D'Aniello M, Tartaglia R, Landolfo R, Jaspart J-P, Demonceau J-F. Seismic pre-qualification tests of EC8-compliant external extended stiffened end-plate beam-to-column joints. Eng Struct 2023;291:116386.
[2] Landolfo R. European seismic prequalification of steel beam-to-column joints: EQUALJOINTS and EQUALJOINTS-Plus projects. J Constr Steel Res 2022;192:107238. https://doi.org/10.1016/j.jcsr.2022.107238.
[3] Tartaglia R, D'Aniello M, Rassati GA, Swanson JA, Landolfo R. Full strength extended stiffened end-plate joints: AISC vs recent European design criteria. Eng Struct 2018;159:155–71.
[4] Mou B, Li X, Bai Y, Wang L. Shear behavior of panel zones in steel beam-to-column connections with unequal depth of outer annular stiffener. J Struct Eng 2019;145(2):4018247.
[5] Tartaglia R, D'Aniello M, Zimbru M, Landolfo R. Finite element simulations on the ultimate response of extended stiffened end-plate joints. Steel Compos Struct Int J 2018;27(6):727–45.
[6] Tartaglia R, D'Aniello M, Rassati GA. Proposal of AISC-compliant seismic design criteria for ductile partially-restrained end-plate bolted joints. J Constr Steel Res 2019;159:364–83.
[7] Almutairi FF, Tsavdaridis KD, Alonso Rodriguez A, Hajirasoulihad I. Expertimental investigation on demountable steel-concrete composite reduced web section (RWS) connections under cyclic loads. Bull. Earthq. Eng. 2023.
[8] Almutairi FF, Tsavdaridis KD, Alonso Rodriguez A, Asteris PG, Lemonis ME. Hysteretic behaviour of composite reduced web section (RWS) connections for seismic applications. J Earthq Eng 2023:1–36.
[9] Tabar AM, Alonso-Rodriguez A, Tsavdaridis KDaniel. Building retrofit with reduced web (RWS) and beam (RBS) section limited-ductility connections. J Constr Steel Res 2022.
[10] Tsavdaridis KD, Lau CK, Alonso-Rodríguez A. Experimental behaviour of non-seismical RWS connections with perforated beams under cyclic actions. J Constr Steel Res 2021;183:106756.
[11] Shaheen MA, Tsavdaridis KD, Yamada S. Comprehensive FE study of the hysteretic behaviour of steel-concrete composite and non-composite RWS beam-to-column connections. J Struct Eng 2018.
[12] Shin M, Kim S-P, Halterman A, Aschheim M. Seismic toughness and failure mechanisms of reduced web-section beams: phase 1 tests. Eng Struct 2017;141:198–216.
[13] Shin M, Kim S-P, Halterman A, Aschheim M. Seismic toughness and failure mechanisms of reduced web-section beams: phase 2 tests. Eng Struct 2017;141:607–23.
[14] Bi R, Jia L, Li P, Wang Q. Multiparameter seismic behavior of castellated beam-to-column connections based on stress migration. Structures 2021;29:1137–53.
[15] Guo J, Shi Q, Li T, Ma G. Mechanical performance of hybrid high-strength steel composite cellular beam under low cyclic loading. J Constr Steel Res 2023;203:107801.
[16] Lagaros ND, Psarras LD, Papadrakakis M, Panagiotou G. Optimum design of steel structures with web openings. Eng Struct 2008;30(9):2528–37.
[17] Chung KF, Liu CH, Ko ACH. Steel beams with large web openings of various shapes and sizes: an empirical design method using a generalised moment-shear interaction curve. J Constr Steel Res 2003;59(9):1177–200.
[18] Tsavdaridis KD, D'Mello C. Vierendeel bending study of perforated steel beams with various novel web opening shapes through nonlinear finite-element analyses. J Struct Eng 2012;138(10):1214–30.
[19] Liu TCH, Chung KF. Steel beams with large web openings of various shapes and sizes: finite element investigation. J Constr Steel Res 2003;59(9):1159–76.
[20] Yang Q, Li B, Yang N. Aseismic behaviors of steel moment resisting frames with opening in beam web. J Constr Steel Res 2009;65(6):1323–36.

[21] Tsavdaridis KD, Pilbin C, Lau CK. FE parametric study of RWS/WUF-B moment connections with elliptically-based beam web openings under monotonic and cyclic loading. Int J Steel Struct 2017;17(2):677–94.
[22] Erfani S, Akrami V. Increasing seismic energy dissipation of steel moment frames using reduced web section (RWS) connection. J Earthq Eng 2017;21(7):1090–112.
[23] Chung KF. Recent advances in design of steel and composite beams with web openings. Adv Struct Eng 2012;15(9):1521–36.
[24] Darwin D. Design of composite beams with web openings. Prog Struct Eng Mater 2000;2(2):157–63.
[25] Zeytinci BM, Şahin M, Güler MA, Tsavdaridis KD. A practical design formulation for perforated beams with openings strengthened with ring type stiffeners subject to Vierendeel actions. J Build Eng 2021;43. https://doi.org/10.1016/j.jobe.2021.102915.
[26] Lawson RM, Hicks SJ. Design of composite beams with large web openings 2011.
[27] Darwin D. AISC design guide 31 steel and composite beams with web openings 1990.
[28] ANSI/AISC 358-16. Prequalified connections for special and intermediate steel moment frames for seismic applications 2016.
[29] ANSI/AISC 341-16. Seismic provisions for structural steel buildings. Seism Provis Struct Steel Build 2016:60601.
[30] CEN. Eurocode 8: design of structures for earthquake resistance-part 1: general rules, seismic actions and rules for buildings. Eur Comm Stand Bruss 2005;(1998).
[31] Erfani S, Akrami V, Mohammad-nejad A. Lateral load resisting behavior of steel moment frames with reduced web section (RWS) beams. Structures 2020;28:251–65.
[32] Erfani S, Akrami V. A nonlinear macro-model for numerical simulation of perforated steel beams. Int J Steel Struct 2019:1–19.
[33] Akrami V, Erfani S. Effect of local web buckling on the cyclic behavior of reduced web beam sections (RWBS). Steel Compos Struct 2015;18(3):641–57.
[34] Davarpanah M, Ronagh H, Memarzadeh P, Behnamfar F. Cyclic behavior of welded elliptical-shaped RWS moment frame. J Constr Steel Res 2020;175:106319.
[35] Boushehri K, Tsavdaridis KD, Cai G. Seismic behaviour of RWS moment connections to deep columns with European sections. J Constr Steel Res 2019;161:416–35.
[36] Tsavdaridis KD, Faghih F, Nikitas N. Assessment of perforated steel beam-to-column connections subjected to cyclic loading. J Earthq Eng 2014;18(8):1302–25.
[37] Tsavdaridis KD, Papadopoulos T. A FE parametric study of RWS beam-to-column bolted connections with cellular beams. J Constr Steel Res 2016;116:92–113.
[38] Naughton DT, Tsavdaridis KD, Maraveas C, Nicolaou A. Pushover analysis of steel seismic resistant frames with reduced web section and reduced beam section connections. Front Built Environ 2017;3:59.
[39] Ferreira FPV, Shamass R, Limbachiya V, Tsavdaridis KD, Martins CH. Lateral–torsional buckling resistance prediction model for steel cellular beams generated by Artificial Neural Networks (ANN). Thin Walled Struct 2022;170:108592.
[40] Degtyarev VV, Tsavdaridis KD. Buckling and ultimate load prediction models for perforated steel beams using machine learning algorithms. J Build Eng 2022;v51:104316.
[41] Chaudhari T, MacRae G, Bull D, Clifton C, Hicks S. Experimental behaviour of steel beam-column subassemblies with different slab configurations. J Constr Steel Res 2019;162:105699.
[42] Ibarra LF, Medina RA, Krawinkler H. Hysteretic models that incorporate strength and stiffness deterioration. Earthq Eng Struct Dyn 2005;34(12):1489–511.
[43] ABAQUS. Abaqus user's manual, version 6.19. Dassault Syst. Simulia Corp., Provid. RI, USA. 2019.
[44] CEN. Eurocode 3: design of steel structures-part 1–1: General rules and rules for buildings 2005.
[45] Tsavdaridis KD, D'Mello C. FE investigation of perforated sections with standard and non-standard web opening configurations and sizes. in: Proceedings of the Sixth International Conference on Advances is Steel Structures 2009.
[46] E. C. for S. CEN, Eurocode 2: design of concrete structures–part 1.1: general rules and rules for buildings; 2004.
[47] Cornelissen HAW, Hordijk DA, Reinhardt H. Experimental determination of crack softening characteristics of normalweight and lightweight. Heron 1986;31(2):45–56.
[48] Shaheen MA. A new idea to improve the cyclic performance of end plate beam–column connections. Eng Struct 2022;253:113759.
[49] Guo B, Wang JT, Liang T, Bao Z. Study on seismic performance of a new type energy dissipation steel moment frames. Appl Mech Mater 2011;94:764–70.
[50] Li B, Yang Q, Yang N. An investigation on aseismic connection with opening in beam web in steel moment frames. Adv Struct Eng 2011;14(3):575–87.
[51] Eladly MM, Schafer BW. Numerical and analytical study of stainless steel beam-to-column extended end-plate connections. Eng Struct 2021;240:112392. https://doi.org/10.1016/j.engstruct.2021.112392.
[52] Zhang X, Zheng S, Zhao X. Seismic performance of steel beam-to-column moment connections with different structural forms. J Constr Steel Res 2019;158:130–42.
[53] Nazaralizadeh H, Ronagh H, Memarzadeh P, Behnamfar F. Cyclic performance of bolted end-plate RWS connection with vertical-slits. J Constr Steel Res 2020;173:106236.
[54] Xu Q, Chen H, Li W, Zheng S, Zhang X. Experimental investigation on seismic behavior of steel welded connections considering the influence of structural forms. Eng Fail Anal 2022;139:106499.
[55] CEN, Eurocode 3: design of steel structures—part 1–8: design of joints—the European Standard EN 1993–1-8: 2005, in European Committee for Standardization, Brussels, no. 1993, 2005.
[56] Elkady A, Lignos DG. Modeling of the composite action in fully restrained beam-to-column connections: implications in the seismic design and collapse capacity of steel special moment frames. Earthq Eng Struct Dyn 2014;43(13):1935–54.
[57] Hedayat AA, Celikag M. Post-Northridge connection with modified beam end configuration to enhance strength and ductility. J Constr Steel Res 2009;65(7):1413–30.
[58] Momenzadeh S, Kazemi MT, Asl MH. Seismic performance of reduced web section moment connections. Int J Steel Struct 2017;17(2):413–25.
[59] Asl MH, Jahanian M. Behaviour of Steel Deep Beams in Moment Frames with Web Opening Subjected to Lateral Loading. Int J Steel Struct 2020;20(5):1482–97.
[60] Fares S, Coulson J, Dinehart D. AISC design guide 31 castellated and cellular beam design 2016.
[61] Özkılıç YO. Cyclic and monotonic performance of unstiffened extended end-plate connections having thin end-plates and large-bolts. Eng Struct 2023;281:115794.